

Xin-Guang Zhu · Govindjee · Neil R. Baker
Eric deSturler · Donald R. Ort · Stephen P. Long

Chlorophyll *a* fluorescence induction kinetics in leaves predicted from a model describing each discrete step of excitation energy and electron transfer associated with Photosystem II

Received: 15 March 2005 / Accepted: 13 June 2005 / Published online: 18 October 2005
© Springer-Verlag 2005

Abstract Chlorophyll *a* fluorescence induction (FI) is widely used as a probe for studying photosynthesis. On illumination, fluorescence emission rises from an initial level O to a maximum P through transient steps, termed J and I. FI kinetics reflect the overall performance of photosystem II (PSII). Although FI kinetics are commonly and easily measured, there is a lack of consensus as to what controls the characteristic series of transients, partially because most of the current models of FI focus on subsets of reactions of PSII, but not the whole. Here we present a model of fluorescence induction, which includes all discrete energy and electron transfer steps in and around PSII, avoiding any assumptions about what is critical to obtaining O J I P kinetics. This model successfully simulates the observed kinetics of fluorescence induction including O J I P transients. The fluorescence emission in this model was calculated directly from the amount of excited singlet-state chlorophyll in the core and peripheral antennae of PSII. Electron and energy transfer were simulated by a series of linked differential equations. A variable step numerical integration procedure (*ode15s*) from MATLAB provided a

computationally efficient method of solving these linked equations. This *in silico* representation of the complete molecular system provides an experimental workbench for testing hypotheses as to the underlying mechanism controlling the O J I P kinetics and fluorescence emission at these points. Simulations based on this model showed that J corresponds to the peak concentrations of $Q_A^-Q_B^-$ (Q_A and Q_B are the first and second quinone electron acceptor of PSII respectively) and $Q_A^-Q_B^-$ and I to the first shoulder in the increase in concentration of $Q_A^-Q_B^{2-}$. The P peak coincides with maximum concentrations of both $Q_A^-Q_B^{2-}$ and PQH₂. In addition, simulations using this model suggest that different ratios of the peripheral antenna and core antenna lead to differences in fluorescence emission at O without affecting fluorescence emission at J, I and P. An increase in the concentration of Q_B^- -nonreducing PSII centers leads to higher fluorescence emission at O and correspondingly decreases the variable to maximum fluorescence ratio (F_v/F_m).

Keywords Photosynthesis · Chlorophyll fluorescence · Model · System biology · *In silico*

X.-G. Zhu · D. R. Ort · S. P. Long (✉)
Department of Plant Biology and Crop Sciences,
University of Illinois at Urbana Champaign,
379 Madigan Laboratory, 1201 W. Gregory Drive,
Urbana, IL 61801, USA
E-mail: stevel@life.uiuc.edu
Tel.: +1-217-3332487
Fax: +1-217-2447563

Govindjee
Department of Plant Biology and Department of Biochemistry,
265 Morrill Hall, 505 S Goodwin Ave, Urbana, IL 61801, USA

N. R. Baker
Department of Biological Sciences, University of Essex,
Colchester, Essex, CO4 3SQ, UK

E. deSturler
Department of Computer Science, 4314 Thomas M. Siebel Center
for Computer Science, University of Illinois at Urbana Champaign,
Urbana, IL 61801, USA

Introduction

When dark-adapted oxygenic photosynthetic cells are illuminated, chlorophyll (Chl) *a* fluorescence shows complex induction kinetics (FI) termed the Kautsky curve. This is characterized by a series of inflections in the rate of rise in the fluorescence level (F) termed the OJIP transient (Strasser et al. 1995, 2004). Each letter denotes a distinct inflection in the induction curve. Chl *a* fluorescence is widely used as a probe for different aspects of photosynthesis since fluorescence measurements are non-invasive, highly sensitive, fast and easily conducted (Bolhár-Nordenkamp et al. 1989; Baker and Oxborough 2004). Furthermore, FI may be measured with relatively inexpensive equipment despite the potential wealth of information generated about the

primary events of photosynthesis (Bolhár-Nordenkamp et al. 1989; Krause and Weis 1991; Govindjee 1995, 2004; Lazar 1999). Since FI varies under different stress conditions, e.g. high light and low temperatures, FI has been used in studying the stress physiology of photosynthesis (Baker et al. 1983; Krause and Weis 1991; Rohacek and Bartak 1999; Sayed 2003).

Fluorescence induction (FI) kinetics reflect the overall performance of photosystem II (PSII) following dark adaptation. Although FI kinetics are commonly and easily measured, there is a lack of consensus as to the underlying mechanisms controlling the characteristic series of transients, perhaps in part because previous models of FI did not include all of the processes involved in excitation energy transduction and photochemistry by PSII. For example, several fluorescence models were constructed to study FI in the presence of 3-(3', 4' -dichlorophenyl)-1,1-dimethylurea (DCMU) or for FI in low light fluxes (Lavergne and Trissl 1995; Vavilin et al. 1998). These models predict the performance of photosynthetic electron transfer reactions to the point of Q_A reduction. Stirbet et al. (1998) calculated the fluorescence emission based on the reduction state of Q_A , not directly from the amount of singlet-excited chlorophylls and the rate constants for different energy dissipation process from singlet-excited Chl as in previous models. Stirbet and Strasser (2001) hypothesized in their model that the accumulation of reduced pheophytin (Pheo) has a key role in FI kinetics (Vredenberg 2000, 2004). Schreiber and Krieger (1996) suggested at variable fluorescence as controlled by decrease in rate of primary charge separation and increase in rate of charge recombination. This is modulated by changes in the rate constant of heat dissipation, nonradiative decay to the ground state from $P_{680}^+Pheo^-$ and spin dephasing resulting in triplet state of the radical pair (P_{680} is the primary electron donor and Pheo is the primary electron acceptor of PSII). Lebedeva et al. (2002) developed a model which simulated FI over a range of light fluxes and incorporated the effect of membrane potentials on the rate constants of various reactions. These two models (Schreiber and Krieger 1996; Lebedeva et al. 2002) did not however include the molecular mechanism of the oxygen evolution complex. A model by Lazar (2003) provided a detailed description of reactions around PSII to simulate FI. However, neither of these models (Lebedeva et al. 2002; Lazar 2003) included the differentiation between core and peripheral antennas in the light harvesting complex of PSII. Collectively, these models (Schreiber and Krieger 1996; Stirbet and Strasser 2001; Lebedeva et al. 2002; Lazar 2003) developed explanations of the FI kinetics based on the assumption that a different single process or subset of processes determines the response.

Here we use an alternative approach, in which all of the discrete steps involved in light capture, excitation energy transfer and electron transfer associated with PSII at both the donor side and the acceptor side are included; i.e. no assumptions are made about what may

be excluded for simplification. We then examine how alteration of individual steps affects the simulated FI curve. In addition to using a complete description of all the energy and electron transfer reactions, our approach describes individually the different components associated with PSII activities, rather than representing them together as intermediate complexes (see Fig. 1). The first objective of this study was to test whether such a complete model can successfully simulate the FI kinetics under normal physiological conditions, e.g. without DCMU. Secondly, this *in silico* representation of the complete system was used to test hypotheses derived from previous models underlying mechanisms controlling FI kinetics. Thirdly, the effects of changes in the rate constants of the excitation energy and electron transfer processes associated with PSII on FI were examined. Finally, the effects of different proportions of PSII Q_B -nonreducing centers on FI were examined.

Materials and methods

The model and the assumptions

A schematic representation of the model is shown in Fig. 1. The whole model is composed of the following major components: peripheral antenna system of PSII, core antenna system of PSII, oxygen evolving complex, PSII reaction center (P_{680} , the primary electron donor of PSII), Pheo (the primary electron acceptor of PSII), the redox-active Tyrosine of the D1 protein, one tightly bound plastoquinone Q_A , and one loosely bound plastoquinone Q_B . Water molecules donate electrons to P_{680}^+ , while the plastoquinol pool is required to exchange with Q_BH_2 and transfer the reducing equivalent to the cytochrome b_6f complex and provide electrons for subsequent electron transfer to PSI (Fig. 1).

The following assumptions are used in our model and underlie the series of equations given in next section :

1. Chl *a* fluorescence (> 80%) is assumed to be emitted from PSII complexes only. Although PSI complexes are weakly fluorescent, variable fluorescence is attributed to PSII only. Antenna chlorophylls however contribute to partitioning of excitation energy (Krause and Weis 1991). Both PSI and PSII units include associated carotenoids (Ben-Shem et al. 2003; Ferreira et al. 2004; Liu et al. 2004) which influence efficiency of photosynthesis in blue light, but not in the red excitation region where they do not absorb. Therefore, without decreasing its predictive ability, carotenoids were not included in our current FI model for simplicity.
2. Zeaxanthin in the thylakoid membrane serves an important photoprotective role through non-photochemical quenching in high light stress (Horton et al. 1996; Niyogi 1999). This non-photochemical quenching occurs at much slower time scale than the photochemical reactions and the electron transfer

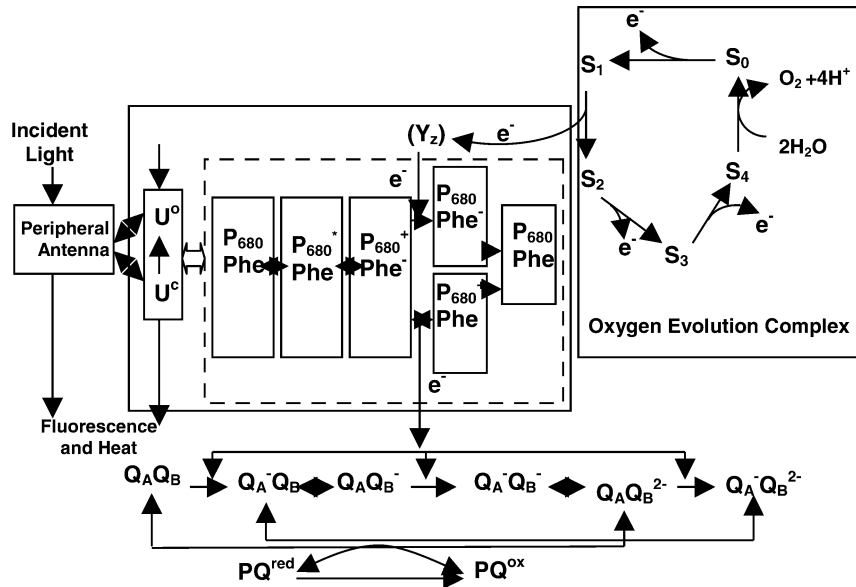


Fig. 1 Block flow diagram of the steps underlying chlorophyll fluorescence induction on a dark-light transition. In this diagram, only the reactions associated with one Q_B -reducing PSII unit is included. Each illustrated component is represented by a differential equation in the model (Appendix 1). Change in the concentration of each component illustrated is achieved by numerical integration of these linked equations. The section enclosed by the dotted line represents the charge separation process in the PSII reaction center. U^o and U^c represent the singlet-excited chlorophylls within the core antenna associated with the open and closed reaction center respectively. S_1 , S_2 , S_3 , and S_4 represent the four redox states of the oxygen evolving complex (OEC). Y_z : primary electron donor for photosystem II reaction center (P_{680}). Phe^- : pheophytin; PQ : plastoquinone; PQH_2 : plastoquinol; Q_A : the first quinone electron acceptor in PSII; Q_B : the second quinone electron acceptor in PSII; Cyt b_6/f : cytochrome b_6/f complex

- reactions during OJIP transients in dark adapted leaves (Horton et al. 1996; Niyogi 1999). Therefore, in the current model, the effects of zeaxanthin on OJIP FI transients are ignored. The zeaxanthin molecules are expected to influence greatly the complete fluorescence induction curve, i.e. phases beyond P, which includes both the increase and the decline of fluorescence in an extended exposure to actinic light.
3. The light harvesting system consists of two distinct types of pigment-protein complexes, i.e. the PSII core antenna system and the peripheral antenna (Horton et al. 1996). In our model, Chl a fluorescence is assumed to be emitted from chlorophyll molecules in both peripheral and core antenna, and excitation energy in core antenna of the closed reaction centers can migrate to the core antenna of open reaction centers with a given probability (Joliot and Joliot 1964; Deprez et al. 1990).
 4. The process of oxygen evolution is assumed to result from a succession of non-interacting oxygen-evolving complexes (OEC) with sequential redox states (Kok et al. 1970; Forbush et al. 1971). These different redox states of OEC are represented as S states (S_n) with the subscript indicating the number of

accumulated oxidizing equivalents or positive charges. When four oxidizing equivalents have been accumulated, an oxygen molecule is evolved, and the S state reset to S_0 and another cycle starts. The transition between each successive state of the oxygen evolving complex requires absorption of the energy of one photon: $S_0 \rightarrow S_1 \rightarrow S_2 \rightarrow S_3 \rightarrow (S_4) \rightarrow S_0 \rightarrow S_1 \dots$. The positive or oxidizing equivalent is obtained from P_{680}^+ via the tyrosine Z (Y_z) of the D1 protein. This model assumes the rate constants of electron transfer reactions from OEC to P_{680}^+ (via Y_z) are the same for each S redox state. Primary charge separation occurs in the PSII reaction center, which generates P_{680}^+ and Phe^- . An electron is transferred from Phe^- to the first plastoquinone electron acceptor Q_A , which in turn reduces Q_B (Vermeglio 1977; Wraight 1977). The times for the transitions of $Q_A^- Q_B \rightarrow Q_A Q_B^-$ and $Q_A^- Q_B^- \rightarrow Q_A Q_B^{2-}$ are assumed to be 150 μs and 400 μs respectively (Bowes and Crofts 1980). Successive linear transfer from S_0 , S_1 , S_2 , S_3 , (S_4) is assumed in this model. The possible misses, double hits, inactivation, backward transitions are not included in the model (Packham et al. 1988; Meunier 1993; Meunier et al. 1996; Quigg et al. 2003). An analytical solution to an extended Kok model which includes possible misses, double hits, inactivation, and backward transitions has been developed (Shinkarev 2005), which holds the potential to be incorporated into our model in the future.

5. After Q_B sequentially receives two electrons from Q_A^- , Q_B becomes fully reduced in the form of Q_B^{2-} which is then protonated to form $Q_B H_2$. For simplicity, we have assumed that protonation of Q_B^{2-} is instantaneous. $Q_B H_2$ exchanges with oxidized plastoquinone (PQ) in the thylakoid membrane. The oxidized plastoquinone binds to the PSII Q_B binding site and reforms Q_B again. PQH_2 in the thylakoid membrane is oxidized through the cytochrome b_6/f complex (Cyt

- b₆f). It is assumed, as in the model of Stirbet et al. (1998), that reactions beyond Cyt b₆f do not affect the fluorescence induction curve.
6. Oxidized PQ is assumed to act as a direct quencher of excitation energy in PSII and not simply as a photochemical quencher; the changes in the redox state of the PQ pool (Vernotte et al. 1979; Kramer et al. 1995) and their effects on fluorescence were included in the model.
 7. A closed reaction center is defined as a PSII reaction center in which the associated Q_A is reduced. Therefore the proportion of open reaction centers (q) is given by:

$$q = \frac{[Q_A]}{[Q_A] + [Q_A^-]} \quad (1)$$

The model assumes a probability parameter p as the likelihood of the migration of excitation energy from the core antenna of a closed reaction center to that of an open reaction center (Joliot and Joliot 1964; Deprez et al. 1990).
 8. Except where noted, all reactions in our model are described using a first order kinetic equation, e.g. the rate of exciton transfer from the peripheral to the core antenna, v_{AU} , is calculated as: $[A_p]k_{AU}$, where $[A_p]$ is the concentration of excited singlet-state chlorophylls located in the peripheral antenna and k_{AU} is the rate constant of excitation energy transfer from the peripheral to the core antenna; the reversible electron transfer between Q_A and Q_B, and the oxidation of plastoquinol in the thylakoid membrane through the cytochrome b₆f complex are assumed to have first-order kinetics, as in the model of Stirbet et al. (1998). The only exception to first order kinetics are the reactions for exchange of plastoquinones, e.g. the exchange of oxidized PQ with Q_AQ_B²⁻ (or Q_AQ_BH₂) are assumed to be second order.
 9. Lebedeva et al. (2002) showed that electric field effects are of consequence to FI only in measurements in low and medium light fluxes. In this study, a saturating photosynthetic photon flux density (PPFD) of 3,000 μmol m⁻² s⁻¹ is to simulate FI; as a result, the influence of the electrical field can be ignored. Therefore, the changes in the rate constants of electron transfer from P₆₈₀ to Q_A and from Q_A⁻ to Q_B upon changes in the electric field across the thylakoid membrane during a dark to light transition are not included.
 10. The net charge of the OEC influences the rate constants of primary charge separation and charge recombination. However, only a minor fraction of PSII are thought to be affected (Dau 1994), therefore the effect of different S states on rate constants of primary charge separation and charge recombination are ignored in our model. Baake and Schloder (1992) have shown that inclusion of other reactions describing electron transfer steps beyond the oxidation of the reduced PQ pool did not

improve model fit to the experimentally recorded FI to P. Therefore, only the reactions prior to PQH₂ oxidation are included in our model.

11. Previous models (Lebedeva et al. 2002; Stirbet et al. 1998; Trissl and Lavergne 1995; Vredenberg 2000) have not accounted for the heterogeneity of PSII, i.e. the Q_B-reducing and Q_B-nonreducing PSII reaction centers, found in nature (Guenther and Melis 1990; Krause and Weis 1991; Melis 1991; Lavergne and Briantais 1996). In our model, the effects of different proportions of Q_B-nonreducing PSII reaction centers are considered. Our model assumes that the Q_B-nonreducing centers have a smaller core antenna compared to Q_B-reducing reaction center, and do not include peripheral antenna (Chylla and Whitmarsh 1990). The Q_B-nonreducing PSII centers are also assumed to have their own OEC, Q_A and Q_B. The chlorophylls detached from core antenna and all the chlorophylls of peripheral antenna of Q_B-nonreducing center are assumed to be separated from Q_B-nonreducing PSII reaction center.

Rate equations describing each excitation/electron transfer reaction

This section describes the rate equations representing the model structure and assumptions in the sequence of excitation energy absorption, excitation energy transfer, charge separation and electron transfer around Q_B-reducing PSII reaction centers. Reactions around Q_B-nonreducing PSII reaction centers use the same rate equations except that the rate constant for electron transfer beyond Q_A is assumed to be zero.

Light absorption by different components of the photosystems

The amount of excitation energy incident on different components of the PSII antenna is determined by the total absorbed excitation energy, the concentration of chlorophylls in different components of PSII units, and the concentration of chlorophylls in PSI units. The PSII unit consists of more than 20 subunits (Hankamer et al. 1997), which are simplified here to one PSII reaction center, one PSII peripheral antenna and two PSII core antenna complexes (Fig. 1). The PSII peripheral antenna complex contains 220 chlorophyll *a* and *b* molecules, and the two PSII core antenna complexes contain about 35 chlorophylls each (Peter and Thornber 1991). Therefore, it is assumed that a PSII unit contains 290 chlorophyll molecules. Similarly, the PSI unit is composed of one PSI core complex with about 96 chlorophylls and one peripheral antenna binding about 80–120 chlorophylls (Chitnis 2001). Consequently, a PSI unit contains 200 chlorophylls in our model. The core antenna of Q_B-nonreducing PSII center is assumed to be

50% of that of a Q_B -reducing PSII center (Chylla and Whitmarsh 1990) and the residual chlorophylls detached from Q_B -nonreducing PSII center dissipated absorbed light energy either as heat or fluorescence. Fifty percent is chosen only to illustrate the effect of a different core antenna size in simulation, rather than as a rigid rule of how these two types of center differ. Assuming the ratio of Q_B -nonreducing to Q_B -reducing PSII reaction center is x , then the chlorophyll content associated with one Q_B -reducing PSII center unit (i.e. one PSII and associated PSI complexes) unit is $(290 + 200n)(1 + x)$. A default value of $n=1$ is used in the current model. Assuming the total incident PPF is I_{in} , the incident PPF on peripheral antenna of Q_B -reducing PSII will be calculated as:

$$I_A = \frac{220I_{in}}{(290 + 200n)(1 + x)}. \quad (2)$$

Similarly, the incident photon flux density on the PSII core antenna of Q_B -reducing PSII unit is:

$$I_c = \frac{70I_{in}}{(290 + 200n)(1 + x)}. \quad (3)$$

The incident photon flux density on the core antenna of Q_B -nonreducing PSII center is calculated similar to Eq. 3 (in Appendix 2).

Excitation energy dissipation as heat and fluorescence

The excitation energy of excited singlet-state chlorophyll is assumed to dissipate through four different pathways: photochemistry, heat, fluorescence, and transfer to other chlorophyll molecules. The rate equations for all four reactions are assumed to follow first-order kinetics (Stirbet et al. 1998). For example, assuming that the concentration of excited singlet-state chlorophylls in the peripheral antenna is A_p , the fluorescence emission (v_{Af}) and heat dissipation (v_{Ad}) from peripheral antenna are calculated as

$$v_{Af} = [A_p]k_f^a; \quad (4)$$

$$v_{Ad} = [A_p]k_d^a; \quad (5)$$

where $[A_p]$ is the concentration of the excited singlet-state chlorophyll in the peripheral antenna of PSII; k_f^a and k_d^a are the rate constants for fluorescence emission and heat dissipation from peripheral antenna respectively.

Excitation energy equilibrium and the primary charge separation reaction

The model assumes that excitation energy of chlorophylls in the core antenna reaches equilibrium instantaneously. The equilibrium between the excitation energy in the antenna chlorophyll of the PSII core complex (Chl^*P_{680}) and the excitation energy in P_{680}

($ChlP_{680}^*$) is represented as $Chl^*P_{680} \leftrightarrow ChlP_{680}^*$. The excited-state energy of different chlorophylls is estimated from the absorption spectrum by:

$$E = \frac{hc}{\lambda_{abs}}, \quad (6)$$

where h is Planck's constant, c is the speed of light, and λ_{abs} is the peak wavelength of light absorbance of certain chlorophyll in our model. An excitation equilibrium is reached when chlorophylls absorbing different wavelengths stay at their excited states with a probability proportional to the Boltzmann factor $\exp[-E_i/kT]$, where E_i is the energy content of the lowest excited-state energy of chlorophyll, T is temperature and k is the Boltzmann constant. Therefore,

$$\frac{[Chl^*P_{680}]}{[ChlP_{680}^*]} = \frac{k_{-t}}{k_t} = \exp\left[\frac{-hc(\lambda_{Chl}^{-1} - \lambda_P^{-1})}{kT}\right]. \quad (7)$$

where k_t is the rate constant of excitation energy transfer from Chl^*P_{680} to $ChlP_{680}^*$, and k_{-t} is the rate constant of excitation energy transfer from $ChlP_{680}^*$ to Chl^*P_{680} . λ_{Chl} and λ_P represent the wavelengths of the maximum absorbance of antenna chlorophyll (678 nm) and reaction center chlorophyll (680 nm) respectively (Schatz et al. 1988). As a simplification, excitation energy absorption by all pigments in the core antenna of PSII was implicitly assumed to follow a normal distribution with a peak wavelength of 678 nm. Light of slightly different wavelengths around 678 nm has essentially the same capacity in carrying out photochemistry. Accessory pigments, e.g. xanthophylls and carotenes, that also exist in PSII units, absorb excitation energy at shorter wavelengths and then transfer excitation energy, via antenna Chl molecules, to P_{680} in an fs to ps time scale (van Grondelle and Gobets 2004).

Equation 7 for calculating the ratio of $[Chl^*P_{680}]$ and $[ChlP_{680}^*]$ does not consider the relative concentration of P_{680} and other chlorophylls in the core antenna. If there are N chlorophylls associated with one P_{680} , the amount of excitation energy reaching P_{680} at equilibrium will decrease gradually with increase in N . Considering both (a) the energy difference and (b) the number of chlorophyll molecules in the PSII core antenna, the amount of P_{680}^* Pheo is calculated as:

$$[P_{680}^*Pheo] = \frac{[U]\left(1 + \frac{k_{-t}}{k_t}\right)^{-1}}{N}, \quad (8)$$

where U represents the total excited singlet-state chlorophylls (including P_{680}^*) in the PSII core antenna. According to Eq. 8, changes in N will lead to changes in the concentration of P_{680}^* Pheo, which will inevitably change the net rate of primary charge separation. This has been confirmed by measurements of the net rates of charge separation for PSII of different antenna size: the higher the N associated with 1 P_{680} , the lower rate of primary charge separation (Holzwarth et al. 1985; Schatz et al. 1987).

The primary charge separation reaction is one of the major pathways for dissipating excitation energy from excited singlet-state PSII reaction center: P_{680}^* .

$$v_1 = q[P_{680}^* \text{Pheo}]k_1^o + [P_{680}^* \text{Pheo}](1-q)(1-p)k_1^c + [P_{680}^* \text{Pheo}](1-q)pk_1^o, \quad (9)$$

$$[P_{680}^* \text{Pheo}] = \frac{[U][P_{680} \text{Pheo}]\left(1 + \frac{k_{-1}}{k_t}\right)^{-1}}{70}, \quad (10)$$

where q is the proportion of open reaction centers in all PSII reaction centers; $[P_{680}^* \text{Pheo}]$ is the concentration of excited singlet-state PSII reaction centers; p is the probability of migration of excitation energy from the core antenna of a closed reaction center to that of an open reaction center, k_1^o is the rate constant of the primary charge separation reaction for open reaction centers; k_1^c is the rate constant of the primary charge separation reaction for closed reaction centers. The rate constants of charge separation in closed (k_1^c) and open reaction center (k_1^o) are different. Seventy is the assumed number of chlorophylls associated with P_{680} in PSII core antenna. The k_1^o is assumed to be $6.2k_1^c$; the rate constant for charge recombination increases by twofold upon the reduction of Q_A (Schatz et al. 1987). These changes in rate constants when Q_A is reduced have been suggested to be the result of (a) altered electrical field by the negative charge on Q_A^- and (b) the shorter distance between Q_A^- and Pheo than from Q_A^- to P_{680} (Dau 1994).

This model assumes that PSII reaction centers are embedded in interconnected photosynthetic units, i.e. they are not isolated from each other (Joliot and Joliot 1964; Deprez et al. 1990). A simple probability parameter (p) ranging from 0 to 1 is used in our model to represent different probabilities of migration of excitation energy from core antennas of closed reaction centers to core antennas of open reaction centers.

The charge recombination reaction

The rate equation for the charge recombination reaction which involves the transfer of electrons from Pheo^- to P_{680}^+ is:

$$v_{-1} = q[P_{680}^+ \text{Pheo}^-]k_{-1}^o + (1-q)[P_{680}^+ \text{Pheo}^-]k_{-1}^c, \quad (11)$$

where, v_{-1} is the charge recombination rate, and k_{-1}^o and k_{-1}^c represent rate constants for the charge recombination reaction between P_{680}^+ and Pheo^- in open and closed PSII reaction centers, respectively.

Excitation energy quenching by P_{680}^+

P_{680}^+ is a quencher of chlorophyll fluorescence (Butler 1972). On a nanosecond to sub-nanosecond scale, the rise of Chl *a* fluorescence after a brief (<1 ns) actinic flash measures the electron flow from tyrosine (Y_2) to P_{680}^+ (Sonneveld et al. 1979). After illumination with a

sequence of short light pulses, oscillation of fluorescence emission with a period of four was observed (Delosme 1971). This phenomena is explained by the hypothesis that the oscillation of electrical fields, which stems from uncompensated positive charges of the OEC, influences the rate of electron transport from the tyrosine residue (Y_2) to P_{680}^+ and correspondingly P_{680}^+ quenching of chlorophyll fluorescence (Dau 1994). In the current model, a rate constant (k_c) of 1 ns^{-1} was used to describe the quenching of Chl *a* fluorescence by P_{680}^+ (Trissl et al. 1993). The quenching of excitation energy in the core antenna is calculated as:

$$v_{P_{680}qU} = [U]([P_{680}^+ \text{Pheo}] + [P_{680}^+ \text{Pheo}^-])k_c, \quad (12)$$

where $[U]$ represents the concentration of excited singlet-state chlorophylls in PSII core antenna.

The quenching of excitation energy in the peripheral antenna is calculated as:

$$v_{P_{680}qA} = [A]([P_{680}^+ \text{Pheo}] + [P_{680}^+ \text{Pheo}^-])k_c, \quad (13)$$

where $[A]$ represents the concentration of excited singlet-state chlorophylls in PSII peripheral antenna (Trissl et al. 1993).

Excitation energy quenching by oxidized plastoquinone

Oxidized plastoquinone is also a strong quencher of chlorophyll fluorescence. Vernotte et al. (1979) found that if all the plastoquinone (PQ) pool is reduced, chlorophyll fluorescence emission is about 10–20% higher than when the PQ pool was oxidized (e.g. with addition of DCMU) under high light. In the current model, the rate constant for plastoquinone quenching is obtained based on the equation for the quantum yield of fluorescence,

$$\Phi_f = \frac{k_f}{k_f + k_d + k_q[\text{PQ}] + k_p[P_{680}Q_A]}, \quad (14)$$

where k_f , k_d , k_q , and k_p represent the rate constants for excitation energy deactivation in the form of fluorescence, heat dissipation, PQ quenching, and quenching by $P_{680}Q_A$ respectively (see reviews: Govindjee 1995, 2004). DCMU blocks electron transfer from Q_A to Q_B ; therefore PQ under high light in the presence of DCMU is in the oxidized state. Assuming Q_A and PQ under high light without DCMU were all in the reduced state, the difference in fluorescence emission under high light with and without DCMU can be used to derive the empirical rate constant of plastoquinone quenching as follows.

In the presence of DCMU, oxidation state of $[PQ]$ is maximal since no electrons are transferred to PQ while k_p is zero, which leads to:

$$\Phi_{f1} = \frac{k_f}{k_f + k_d + k_q[\text{PQT}]}, \quad (15)$$

Table 1 Parameters used in the model of fluorescence induction

Description	Abbr.	Typical value	Reference
Incident photon flux density	I_{in}	3,000 $\mu\text{mol m}^{-2} \text{s}^{-1}$	
The probability of the migration of excitation energy from core antenna of closed reaction centers to that of open reaction centers	p	0–1	Empirical parameter for our model
Speed of light	c	$3 \times 10^8 \text{ m s}^{-1}$	
Planck's constant	h	$6.62 \times 10^{-34} \text{ J s}$	
Boltzmann constant	k	$1.38 \times 10^{-23} \text{ J K}^{-1}$	
Rate constant of electron transfer from Pheo ⁻ to Q _A	k_2	$2 \times 10^9 \text{ s}^{-1}$	Roelofs et al. (1992)
Rate constant of the exchange of PQ with Q _B ²⁻	k_3	800 s^{-1}	Joliot et al. (1992) and Crofts et al. (1993)
Rate constant of electron transfer from Q _A ⁻ to Q _B	k_{AB1}	$2,500 \text{ s}^{-1}$	Bowes and Crofts (1980), Bowes et al. (1980), Robinson and Crofts (1983), Crofts et al. (1993), Haumann and Junge (1994)
Rate constant of electron transfer from Q _A ⁻ to Q _B ⁻	k_{AB2}	$3,300 \text{ s}^{-1}$	Bowes and Crofts (1980), Bowes et al. (1980), Robinson and Crofts (1983), Crofts et al. (1993), Haumann and Junge (1994)
Rate constant of heat dissipation in peripheral antenna system	k_{d}^{a}	10^8 s^{-1}	Trissl and Lavergne (1995)
Rate constant for fluorescence emission from peripheral antenna	k_{f}^{a}	$3 \times 10^7 \text{ s}^{-1}$	Lavergne and Trissl (1995) and Brody (2002)
Rate constant of excitation energy transfer from core antenna to peripheral antenna	k_{UA}	10^{10} s^{-1} *	Model estimate (cf. Laible et al. 1994)
Rate constant of electron transfer from Q _B ⁻ to Q _A	k_{BA1}	175 s^{-1}	Bowes et al. (1980) and Lazar (1999)
Rate constant of electron transfer from Q _B ⁻ to Q _A ⁺	k_{BA2}	250 s^{-1}	Diner (1977) and Lazar (1999)
Rate constant of excitation energy quenching by P ₆₈₀ ⁺	k_{c}	$10^9 \text{ s}^{-1} (\mu\text{mol m}^{-2})^{-1}$	Trissl et al. (1993)
Rate constant of charge recombination between Pheo ⁻ and P ₆₈₀ ⁺ in closed PSII reaction centers	$k_{\text{c-1}}^{\text{c}}$	$9 \times 10^8 \text{ s}^{-1}$	Roelofs et al. (1992)
Rate constant of charge separation of closed PSII reaction centers	k_{c1}^{c}	$4 \times 10^9 \text{ s}^{-1}$	Roelofs et al. (1992)
Equilibrium constant for electron transfer between Pheo and Q _A	K_{e}	10^6	Model estimate (cf. Lazar 1999)
Rate constant of transition from S ₀ to S ₁ state	k_{o01}	50 s^{-1}	Dekker et al. (1984)
Rate constant of charge recombination between Pheo ⁻ and P ₆₈₀ ⁺ in open PSII reaction center	$k_{\text{c-1}}^{\text{o}}$	$3 \times 10^8 \text{ s}^{-1}$	Roelofs et al. (1992)
Rate constant of transition from S ₁ to S ₂ state	k_{o12}	$30,000 \text{ s}^{-1}$	Dekker et al. (1984)
Rate constant of transition from S ₂ to S ₃ state	k_{o23}	$10,000 \text{ s}^{-1}$	Dekker et al. (1984)
Rate constant of transition from S ₃ to S ₀ state	k_{o30}	$3,000 \text{ s}^{-1}$	Dekker et al. (1984)
Rate constant of charge separation in open PSII reaction center	k_{o1}^{o}	$2.5 \times 10^{10} \text{ s}^{-1}$	Roelofs et al. (1992)
Rate constant of PQH ₂ oxidation	k_{ox}	$50\text{--}500 \text{ s}^{-1}$	Haehnel (1976), Bouges Bocquet (1977), Whitmarsh et al. (1982), Mitchell et al. (1990)
Rate constant of excitation energy quenching by oxidized plastoquinone	k_{q}	$3 \times 10^6 \text{ s}^{-1} (\mu\text{mol m}^{-2})^{-1}$	Model estimate (cf. Lazar 2003)
Rate constant of the exchange of PQH ₂ with Q _B	k_{r3}	$80\text{--}800 \text{ s}^{-1}$	Golbeck and Kok (1979) and Crofts et al. (1984)
Rate constant of excitation energy transfer from core antenna to reaction center of PSII	k_{t}	s^{-1}	Implicit
Rate constant of excitation energy transfer from reaction center to core antenna of PSII	$k_{\text{-t}}$	s^{-1}	Implicit
Rate constant of excitation energy transfer from peripheral antenna to core antenna of PSII	k_{AU}	10^{10} s^{-1} *	Model estimate (cf. Laible et al. 1994)
Rate constant of heat dissipation in core antenna associated with closed PSII reaction centers	k_{d}^{Uc}	10^8 s^{-1}	Roelofs et al. (1992) and Lazar and Pospisil (1999)
Rate constant for fluorescence emission from core antenna of PSII	k_{f}^{U}	$3 \times 10^7 \text{ s}^{-1}$	Lavergne and Trissl (1995) and Brody (2002)
Rate constant of heat dissipation in core antenna associated with open PSII reaction centers	k_{d}^{Uo}	0.00 s^{-1}	Roelofs et al. (1992)
Rate constant of electron transfer from oxygen evolution complex to P ₆₈₀ ⁺	k_{z}	$5 \times 10^6 \text{ s}^{-1}$	Brettel et al. (1984) and Meyer et al. (1989)
The number of chlorophylls in the core antenna of an Q _B -reducing PSII reaction center	N	70	Peter and Thornber (1991)
Temperature	T	298 K	

Table 1 (Contd.)

Description	Abbr.	Typical value	Reference
The peak wavelength of light absorbance of chlorophyll in PSII reaction center	λ_P	680 nm	Schatz et al. (1988)
The peak wavelength of light absorbance of certain chlorophyll	λ_{abs}	Dependent on the location of the chlorophyll	
The peak wavelength of light absorbance of chlorophyll in core antenna	λ_{Chl}	673 nm	Schatz et al. (1988)

* Estimated value based on the rate of excitation energy transfer between chlorophylls

where [PQT] represents the concentration of the PQ pool assuming all plastoquinone is reduced under strong light. Without DCMU, [PQ] and [Q_A] are zero, which leads to:

$$\Phi_{f2} = \frac{k_f}{k_f + k_d}. \quad (16)$$

Considering that fluorescence emission is about 15% higher in the presence of DCMU than without (Vernotte et al. 1979), empirically then:

$$k_q = \frac{0.15(k_f + k_d)}{[PQT]}. \quad (17)$$

The rate equation for quenching of excitation energy in the core antenna by oxidized plastoquinone is calculated as:

$$v_{PQqU} = [U][PQ]k_q. \quad (18)$$

The rate equation for calculating the quenching of excitation energy in peripheral antenna by oxidized plastoquinone is calculated as:

$$v_{PQqA} = [A][PQ]k_q. \quad (19)$$

Reactions of the oxygen evolving complex

The oxidized PSII reaction center, P₆₈₀⁺, is reduced by Y_z of D1 protein. In this model, it is assumed that electrons pass through Y_z instantaneously. Therefore, electrons from different S states of oxygen evolution complex are assumed to reach directly to P₆₈₀⁺Pheo or P₆₈₀⁺Pheo⁻. For example, the rate of electron transfer from S₁ state of OEC to P₆₈₀⁺Pheo⁻ was calculated as:

$$v_{1z-1} = \frac{[S_{1T}]k_z[P_{680}^+Pheo^-]}{[P_{680}PheoT]}, \quad (20)$$

where k_z is the rate constant of electron transfer from Y_z to P₆₈₀⁺, which is used here as the rate constant for electron transfer from OEC to P₆₈₀⁺; [S_{1T}] is the concentration of OEC in S₁ state before donating electron to P₆₈₀⁺. [P₆₈₀PheoT] represents the total concentration of different states of P₆₈₀Pheo in PSII. The conversion between different consecutive S states of the OEC assumes first-order kinetics.

Reduction of Q_A

Reduced pheophytin reduces the electron acceptor Q_A. A first-order rate equation is used to describe this process. For example, electron transfer from P₆₈₀⁺Pheo⁻ to Q_A was calculated as:

$$v_{2-1} = [P_{680}^+Pheo^-]k_2q, \quad (21)$$

where k₂ is the rate constant for this reaction. Our model incorporates the reverse electron transfer reaction from Q_A⁻ to Pheo using a pseudo-first-order rate equation. For example, the electron transfer rate from Q_A⁻Q_B to Pheo associated with P₆₈₀⁺ was calculated as:

$$v_{r2-01-1} = \frac{[Q_A^-Q_B]k_2[P_{680}^+Pheo]}{Ke[P_{680}PheoT]}, \quad (22)$$

where Ke is the equilibrium constant for the electron transfer between Q_A and Pheo.

Exchange of plastoquinone

The exchange of plastoquinone between the Q_B site and the thylakoid membrane was calculated based on both the concentration of Q_B²⁻ and the redox state of plastoquinone pool in the thylakoid membrane, i.e.

$$v_3 = \frac{[Q_AQ_B^{2-}]k_3[PQ]}{[PQT]}, \quad (23)$$

where k₃ is the rate constant of the exchange.

Fluorescence emission

The total fluorescence emission from both the peripheral antenna and the core antenna complex is calculated as:

$$F = k_f^a A_p + ([U] + [U_i])k_f^u + k_f^a [A_{ip}] + k_f^u [U_{ifc}], \quad (24)$$

where k_f^a and k_f^u are the rate constants for fluorescence emission at the peripheral and core antenna respectively and F is the total fluorescence emission. [U_i] is the concentration of excited singlet-state chlorophylls (including P₆₈₀^{*}) in the core antenna associated with Q_B-nonreducing PSII center. [A_{ip}] is the concentration of excitation energy on peripheral antenna of Q_B-nonre-

ducing PSII. $[U_{ifc}]$ is the concentration of excitation energy on chlorophylls detached from core antenna of Q_B -nonreducing PSII.

Numerical simulation

The rate of change of the concentration of each discrete reduction state of each intermediate or component in PSII is represented by a differential equation. A differential equation for a component is derived by subtracting the sum of all rates consuming this component from the sum of all rates generating the component. All the differential equations, describing rates of concentration change of all intermediates in the photosystem, form a system of linked differential equations. This system of differential equations for the model is listed in Appendix 1. The rate equations used in deriving the system of differential equations are described in the preceding section (*Rate equations describing each excitation/electron transfer reaction*) and listed in Appendix 2. This system of differential equations was solved by numerical integration using a variable order solver algorithm based on multistep numerical differentiation formulae (*ode15s* of MATLAB, Mathworks, Inc. version 6, Natick, MA; Shampine and Reichelt 1997). This algorithm proved the most computationally efficient in dealing with this set of stiff differential equations. Estimates of the kinetic parameters were obtained from the literature as listed in Table 1. The “average” concentrations of intermediates in the light reactions in dark-adapted C_3 leaves were used to initialize the model. It was assumed that all Q_A , Q_B , and plastoquinone are in an oxidized state in dark-adapted leaves.

In this study, the model simulated FI was compared to a typical measured FI curve, assuming all reaction centers are Q_B -reducing PSII centers. Then the origins of different phases of FI were explored by comparing the fluorescence emission to the concentrations of different intermediates or compounds of the photosystem. Thirdly the effects of modifying kinetic and structural parameters of PSII units on FI were studied. Finally, the influences of different proportions of Q_B -nonreducing PSII centers on FI were explored.

Results

Comparison of *in silico* and *in vivo* FI

Accepting the assumptions used in our model, when all discrete reactions of electron transfer from water-splitting through to Cyt b_6f reduction are included, a realistic FI is simulated and several properties apparently determining the O J I P transients emerge. The multiphasic Chl a fluorescence induction curve predicted from the model when a leaf is excited with 3,000 μmol

photons $\text{m}^{-2} \text{s}^{-1}$ mimics the experimentally recorded multiphasic O J I P transients (Fig. 2). This model provides a new basis for extracting more information from the easily measured fluorescence induction transients (Table 2). The predicted fluorescence emission and the reduction status of Q_A do not change at the same rate (Fig. 3). Under a PPFD of 3,000 $\mu\text{mol} \text{m}^{-2} \text{s}^{-1}$, Q_A approaches complete reduction much earlier than the predicted peak value of fluorescence emission (Fig. 3) and the predicted fluorescence emission and the reduction status of Q_A do not change at the same rate.

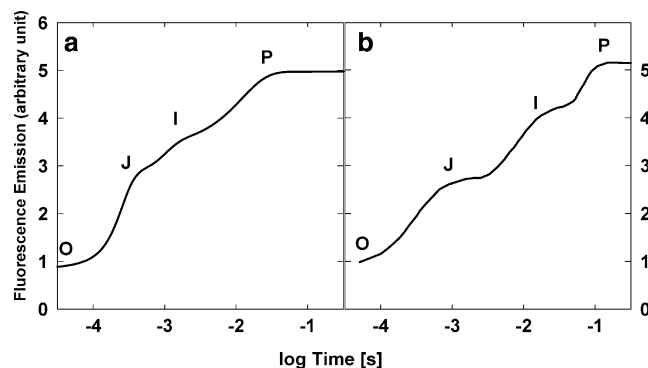


Fig. 2 The fluorescence emission predicted by the current model (a) compared to the experimentally recorded fluorescence induction curve (b, Strasser et al. 1995, 2004). The x axis is the logarithm of time with time using second as unit. The input photon flux density (PPFD) used for the simulation is 3,000 $\mu\text{mol} \text{m}^{-2} \text{s}^{-1}$ (sunlight). The kinetic parameters used in the simulation are listed in Table 1. The initial concentrations of different electron carrier in the dark were assumed to be: a Q_A and Q_B are completely oxidized; b photosystem II reaction centers are all in $P_{680}Phe$ state; c oxygen evolution complexes are in the state of either S_1 or S_0 with a ratio of 4:1; d the ratio of PQ: PQH_2 in thylakoid membrane is 1:1. In the simulation, all PSII reaction centers are assumed to be Q_B -reducing PSII centers. The radiant flux used in the experiment was 600 $\text{W} \text{m}^{-2}$ (Strasser et al. 1995), which corresponds to a photon flux density of 3,255 $\mu\text{mol} \text{photons} (\lambda = 650 \text{ nm}) \text{m}^{-2} \text{s}^{-1}$

Table 2 A summary of the origins and major influencing factors of different inflection points

Inflection point	Origin and major influencing factors
O	Influenced by the relative size of core antenna and peripheral antenna of PSII reaction center
J	Corresponds most closely to the peak concentrations of $Q_A Q_B^-$ and $Q_A^- Q_B^-$
I	Corresponds most closely to the first shoulder of the concentration change of $Q_A^- Q_B^-$
P	Corresponds most closely to the peak concentrations of $Q_A^- Q_B^-$ and PQH_2

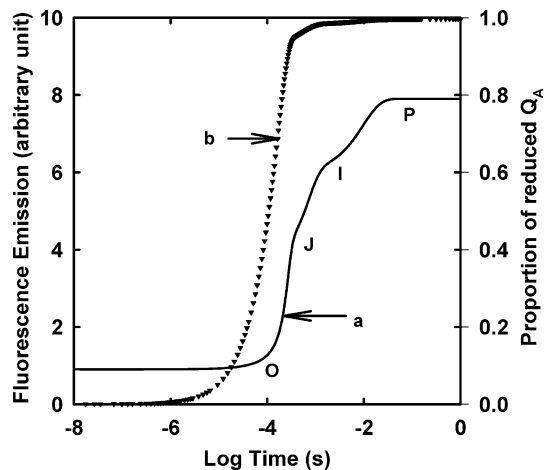


Fig. 3 The predicted fluorescence induction curve (a) and the corresponding proportion of reduced Q_A (b). The x axis is the logarithm of time with time using second as unit. The proportion of reduced Q_A is calculated as: $[Q_A^-]/([Q_A] + [Q_A^-])$; where $[Q_A] = [Q_A^-Q_B^-] + [Q_A^-Q_B] + [Q_A^-Q_B^{2-}]$ and $[Q_A^-] = [Q_A^-Q_B^-] + [Q_A^-Q_B] + [Q_A^-Q_B^{2-}]$. The input photon flux density and simulation conditions are as Fig. 2

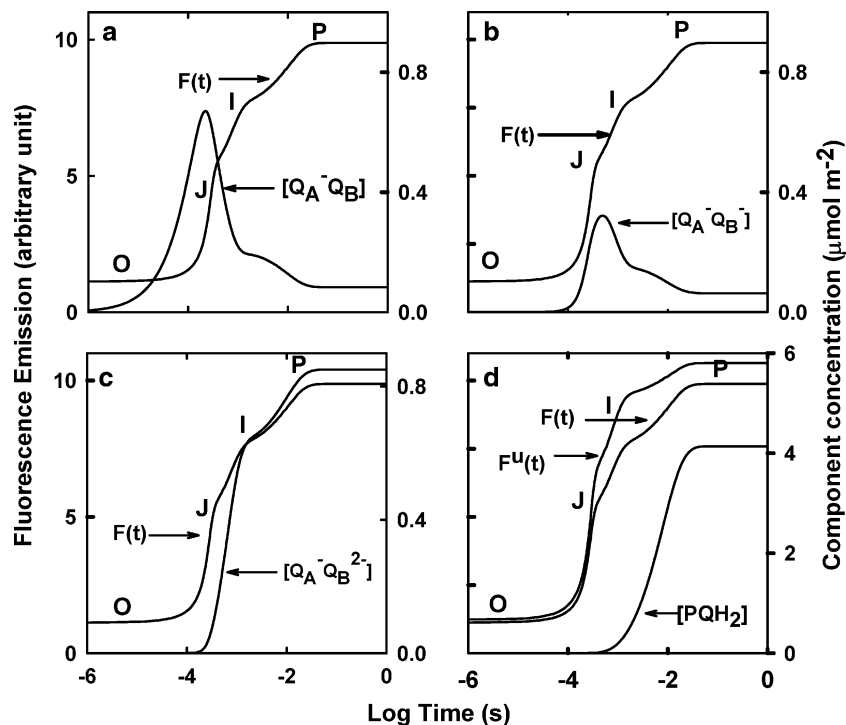
OJIP in relation to the kinetics of intermediate redox states

As suggested by previous theoretical models (Stirbet et al. 1998; Lebedeva et al. 2002; Lazar 2003), the different phases of FI coincide with peak concentrations of oxidized or reduced forms of different components in the electron transfer chain. However, these previous models had developed explanations of the FI kinetics based on the assumption that a different single process

(or subset of processes) determines the response. Our new model (1) assumes equilibrium of excitation energy among all the light harvesting and reaction center pigments; (2) assumes reversible radical pair formation; (3) considers both the acceptor side and donor side reactions of PSII and PSII heterogeneity; and (4) calculates chlorophyll fluorescence based on the concentrations of different fluorescence-emitting excited state forms. Simulations using this improved model were used to relate the phases in FI to the concentrations of different intermediates in electron transfer. Results showed that J coincides with the peak concentrations of $Q_A^-Q_B^-$ and $Q_A^-Q_B$; I with the first shoulder of $Q_A^-Q_B^{2-}$ concentration, and P with the peak concentrations of both $Q_A^-Q_B^{2-}$ and PQH_2 (Fig. 4).

With this detailed description of the different processes and parameters influencing FI, our model was used to examine the effects of modifying structural and

Fig. 4 The predicted fluorescence emission and the corresponding changes in the concentrations of different components involved in the primary events of PSII. The different phases of FI correspond to peak concentrations of different compounds. The phase J, I, and P correspond most closely to the peak concentrations of $Q_A^-Q_B^-$ and $Q_A^-Q_B$, to the first shoulder of the concentration change of $Q_A^-Q_B^{2-}$, and to the peak concentrations of $Q_A^-Q_B^{2-}$ and PQH_2 respectively. The x axis is the logarithm of time and the unit for time is second. The input photon flux density and simulation conditions were as in Fig. 2. The components plotted in these four panels are sequentially, a $Q_A^-Q_B^-$; b $Q_A^-Q_B$; c $Q_A^-Q_B^{2-}$; d PQH_2 . PQ is a strong quencher of fluorescence (Vernote et al 1979); therefore, simulation results with and without PQ quenching are compared. In panel d, the fluorescence emission assuming no PQ quenching, is also included as indicated as $F^u(t)$. The fluorescence emission with PQ quenching is represented as $F(t)$



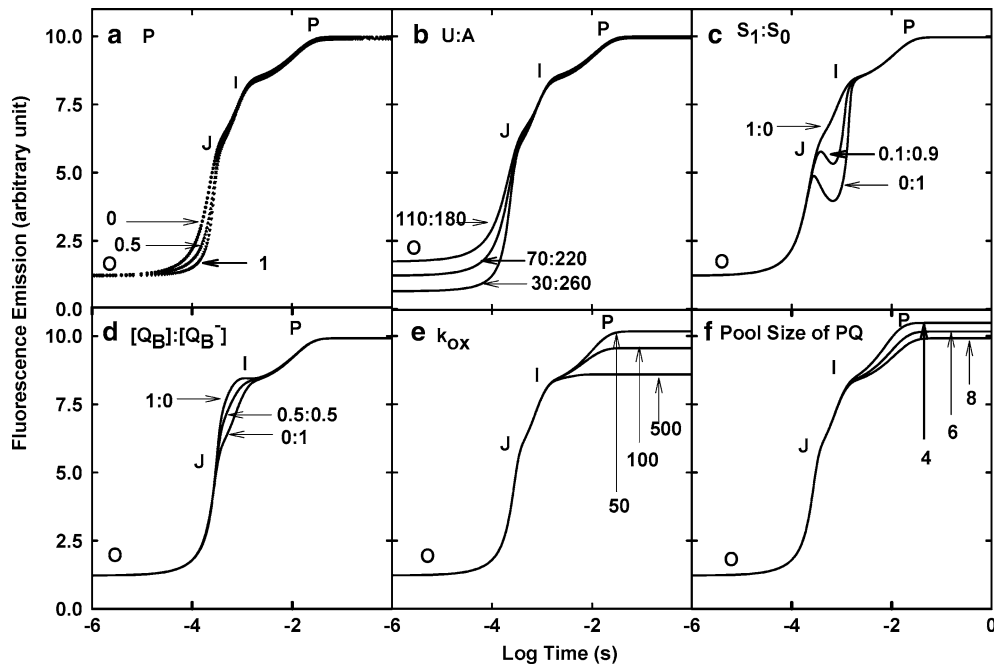


Fig. 5 The predicted influences of different structural and kinetic parameters on the shape of the fluorescence induction curve. The input photon flux density and simulation conditions were as in Fig. 2. The modified structural and kinetic parameters which reflect natural variations in those parameters are: **a** Probability of excitation transfer from core antenna of closed reaction centers to that of open reaction centers; **b** the ratio of the number of chlorophylls in core antenna to that in peripheral antenna; **c** the ratio of the initial concentration of S_1 state to S_0 state of the oxygen evolution complex; **d** the ratio of initial concentration of Q_B to initial concentration of Q_B^- ; **e** the rate constant of PQH_2 oxidation; **f** the pool size of plastoquinone (PQ) in thylakoid membrane

kinetic parameters on FI. The simulations showed that several factors influence the magnitude and shape of FI kinetics. The probability of excitation energy migration from the core antenna of closed reaction centers to the core antenna of open reaction centers ranges from 0.5 to 0.7 (Joliot and Joliot 2003). To account for the natural variation in this number, FI was simulated with a probability of migration of 0, 0.5, and 1. Increasing the probability of excitation transfer from the core antenna of closed reaction centers to the core antenna of open reaction centers progressively delayed the fluorescence increase from O to J without changing fluorescence emission at O (Fig. 5a). Increasing the size of the peripheral antenna relative to the core antenna leads to lower fluorescence emission, and heat dissipation at O (Fig. 5b). By increasing the initial concentration of S_0 , the simulated J becomes more sharply defined. If OEC is assumed to be entirely in the S_0 state on illumination, FI shows a dip after J (Fig. 5c). To further identify the origin of the dip after J, FI was simulated without P_{680}^+ quenching of fluorescence. The result showed that the dip after J was eliminated if P_{680}^+ quenching of fluorescence was ignored (Fig. 6a, b). The fluorescence emission at J gradually increases and finally reaches I when

the initial state of $Q_B:Q_B^-$ is lowered from 1:0 to 0:1 (Fig. 5d). Increasing the rate constant of plastoquinone oxidation (k_{ox}) and the PQ pool size in the thylakoid membrane decreases fluorescence emission at P (Fig. 5e and 5f).

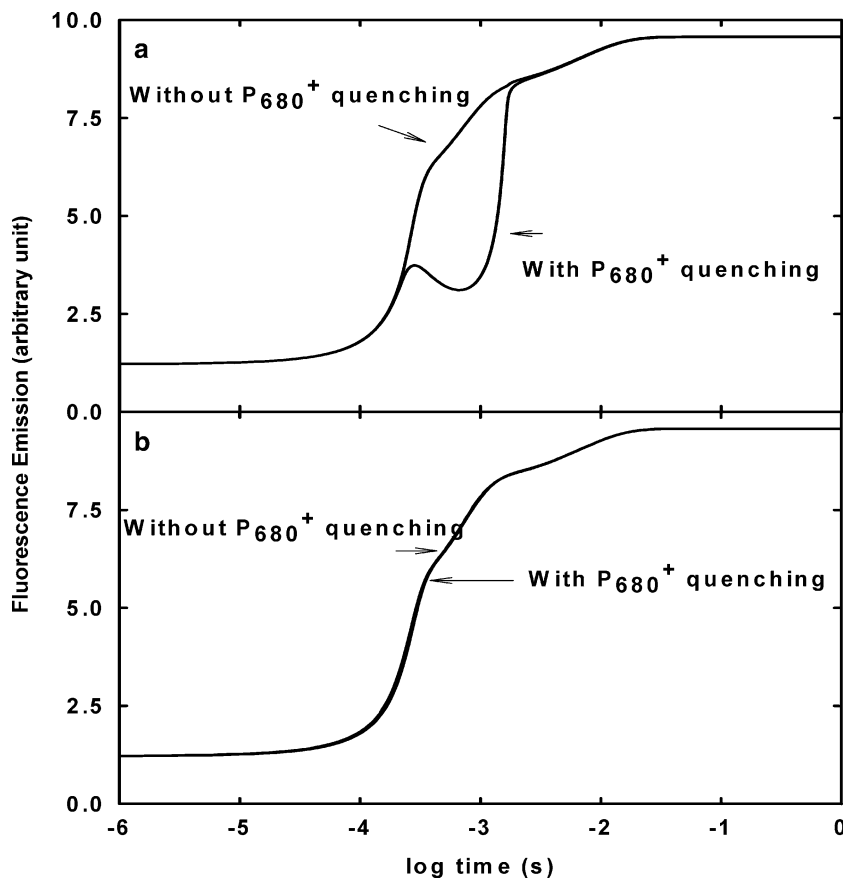
The effects of Q_B -nonreducing PSII centers on FI

Further, we examined the effects of Q_B -nonreducing PSII centers on FI by varying the proportion of Q_B -nonreducing PSII centers at illumination. Assuming the core antenna of a Q_B -nonreducing PSII center is half of that of a Q_B -reducing PSII center (Chylla and Whitmarsh 1990), increasing the proportion of Q_B -nonreducing reaction centers increased the fluorescence emission at O phase (Fig. 7a). The simulated F_v/F_m decreased linearly with increase in the proportion of Q_B -nonreducing PSII (Fig. 7b).

Discussion

The results show that a model including each discrete step in excitation energy/electron/proton transfer around PSII can simulate a realistic Kautsky curve. By sequential alteration of each step quantitative associations with the OJIP transients were revealed. Simulations based on this model showed that J corresponded to the peak concentrations of $Q_A^-Q_B$, $Q_A^-Q_B^-$ and I to the first shoulder in the increase in concentration of $Q_A^-Q_B^-$. The P peak coincided with maximum concentrations of both $Q_A^-Q_B^-$ and PQH_2 . Simulations also suggest that different ratios of the peripheral:core antenna lead to differences in fluorescence emission at O without affecting fluorescence emission at J I and P. Further-

Fig. 6 The predicted fluorescence induction curve with and without quenching by P_{680}^+ . The condition used for simulations were same as in Fig. 2. The simulations were done for two different initial $[S_1]:[S_0]$ of oxygen evolution complexes **a** $[S_1]:[S_0] = 0.1:0.9$; **b** $[S_1]:[S_0] = 0.8:0.2$). There was no detectable difference between the shapes of fluorescence induction curves regardless of whether P_{680}^+ quenching is or is not included if the initial ratio of S_1 to S_0 is 0.8:0.2



more, increased Q_B -nonreducing PSII center increase fluorescence emission at O, decreasing F_v/F_m .

Based on concentrations of intermediates of dark adapted leaves and rate constants for redox reactions and exciton transfer taken from the literature, this model predicts the multi-phasic Chl *a* FI curve (Fig. 2a), including the distinct O J I P transients, closely mimicking observed FI kinetics (Fig. 2b). The current model is distinguished from previous models by its incorporation of each discrete step of energy and electron transfer around PSII. In addition, it differs from some previous models in that it uses the excited singlet-state chlorophyll molecules to predict fluorescence emission (Fig. 1). Furthermore, inclusion of the structural information for the core and the peripheral antenna enables the model to (a) use PFD directly as an input rather than using the rate of Q_A reduction (Stirbet et al. 1998), or the rate of excitation state formation (Lebedeva et al. 2002; Lazar 2003); and to (b) examine the effect of different antenna structures on FI, which was not possible in the previous models (Table 3). Our model assumed that all the reaction centers are open on illumination, and predicts that fluorescence emission at O occurs before any reduction of Q_A (Fig. 3). This shows that FI is not synchronized with Q_A reduction. Specifically the peak concentration of $[Q_A^-]$ does not coincide with P as has been assumed in previous models (Stirbet et al. 1998). This demonstrates the necessity of calculating fluores-

cence emission directly from the concentration of excited singlet-state chlorophyll rather than using the relative reduction state of Q_A to infer fluorescence emission. The fluorescence emission not only reflects changes in the Q_A reduction state, but also the reduction state of Q_B and PQ (Fig. 4); especially PQ which is a strong quencher of fluorescence (Vernotte et al. 1979).

The appearance of J was found to coincide most closely with the maximum concentrations of $Q_A^-Q_B^-$ and $Q_A^-Q_B^{2-}$ (Fig. 4). This result is consistent with the experimental and theoretical results showing that the O-J phase is largely driven by primary photochemistry, i.e. reduction of the primary electron acceptor in PSII, pheophytin, and the first quinone electron acceptor of PSII, Q_A (Delosme 1967; Neubauer and Schreiber 1987; Strasser et al. 1995; Lazar et al. 1997, 1998; Stirbet et al. 1998; Strasser et al. 2004). Consistent with the model of Stirbet et al. (1998), the inflection point I was found to correspond to the first inflection in the concentration of $Q_A^-Q_B^{2-}$ (Fig 4c). The concentration of $Q_A^-Q_B^{2-}$ was maximal at P (Fig. 4c). At the same time, the plastoquinone pool was also maximally reduced at point P (Fig. 4d). Models of FI lacking a description of the electron transfer reactions beyond Q_A reduction, i.e. the Q_B reduction and plastoquinone reduction reactions, fail to simulate the I-P phase (Trissl and Lavergne 1995; Schreiber and Krieger 1996; Vredenberg 2000). Therefore, the appearance of the I-P phase requires the

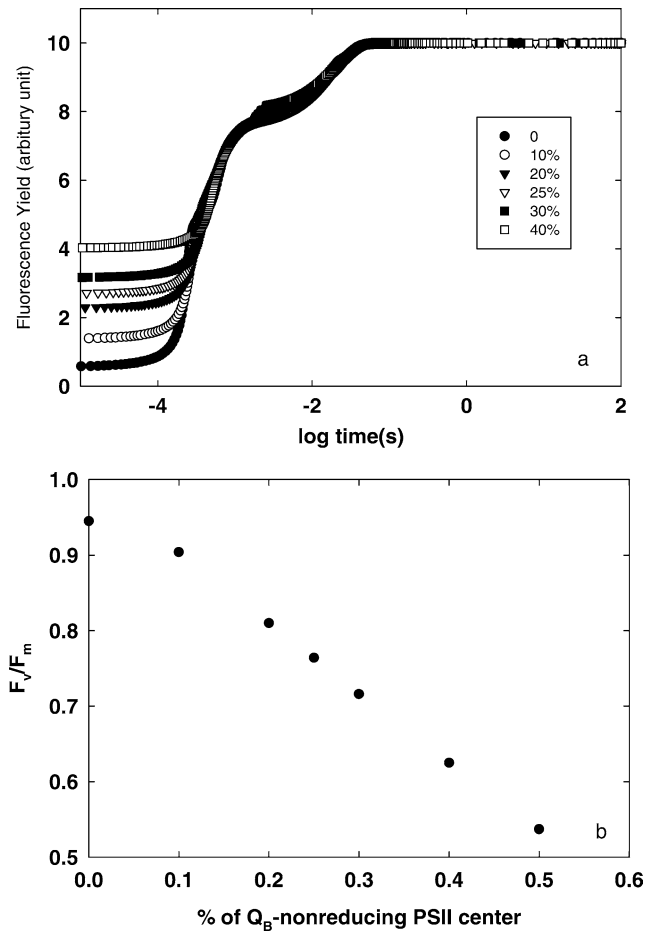


Fig. 7 The effects of the percentage of Q_B-nonreducing PSII reaction center ($x/(1+x)$ with x being the ratio of Q_B-nonreducing to Q_B-reducing PSII reaction center) on (a) fluorescence induction curve and (b) F_v/F_m , or $(F_m - F_o)/F_m$ where F_m and F_o are the fluorescence emission at P and O phase respectively obtained from Fig. 7a. The input photon flux density and simulation conditions used for simulations were the same as in Fig. 2. The maximum fluorescence emission is scaled to be the same level

accumulation of double-reduced Q_B and the reduced plastoquinone pool molecules.

In our model the connectivity between closed and open reaction centers is described using a simple empirical probability parameter p (Eq. 9). With a higher p value, the connectivity between open and closed reaction centers is higher. As in the model of Stirbet et al. (1998), increasing p gradually delays the fluorescence increase from O to J without changing emission at O. This is due to a higher proportion of excitation energy being used in photochemistry with less dissipated as heat and fluorescence when connectivity is higher. Following this rationale, a higher connectivity might imply higher light utilization efficiency for leaves under medium to high light conditions, where some PSII reaction centers are closed. Further, at high light flux, excited chlorophylls in core antenna of closed reaction centers can potentially generate reactive radicals leading to photoinhibition

(Long et al. 1994). Increased connectivity would be partially protective, diverting more excitation energy to photochemistry; this is similar to the photoprotective role of nonphotochemical quenching by diverting more excitation energy for heat dissipation (Horton et al. 1996; Niyogi 1999; Zhu et al. 2004). In contrast to the O-J phase, the fluorescence intensities in the I-P phase are not detectably influenced by p within the current model, which differs from the predictions of the model of Stirbet et al. (1998).

Simulations with the current model suggest that the “structure” of the light harvesting complex influences F_o without apparent changes in fluorescence emission at points J, I and P. A relatively greater peripheral antenna compared to core antenna leads to lower F_o (Fig. 5b). This result provides another mechanism to alter the commonly used fluorescence parameter, F_v/F_m , where $F_v = F_m - F_o$ and F_m is the maximum fluorescence emission under saturating light. Based on this result, F_v/F_m can be altered through changes in the relative size of core antenna and peripheral antenna without any change in the rate constant of charge separation in the PSII reaction center. Specifically, a relatively greater size of peripheral antenna compared to core antenna might be preferred for higher efficiency of excitation energy utilization (Fig. 5b). In this respect, it is interesting to note that the amount of chlorophyll in the peripheral antenna is nearly three times or more than that in the core antenna (Peter and Thornber 1991; Horton et al. 1996). This suggests a potential approach of genetic manipulation of antenna structures, i.e. decreasing the ratio of the size of core antenna to that of peripheral antenna, to increase excitation energy utilization efficiency for leaves of shade environments, e.g. leaves of understory plants or leaves in the lower layers of canopy.

In agreement with the findings of Stirbet et al. (1998), increase in the initial concentration of S_0 , causes J and a subsequent dip to become more pronounced (Fig. 5c). Considering the differences in the rate of transitions between different states of the OEC, especially the slow transition between S_0 and S_1 , relative to other steps, Lazar (2003) has suggested that the dip after I reflects a momentary accumulation of P_{680}^+ , which is a strong quencher of fluorescence. This is confirmed in our simulations: (a) ignoring P_{680}^+ quenching of fluorescence eliminates the dip after point J in FI even when the initial concentration of S_0 is high (Fig. 6a); (b) a high initial concentration of S_1 , instead of S_0 , eliminates the dip after point J because the transition between S_1 and S_2 is fast enough to provide electrons to P_{680}^+ , preventing accumulation of P_{680}^+ and correspondingly the quenching of fluorescence by P_{680}^+ (Fig. 6b). The $S_1:S_0$ ratio for dark-adapted leaves has been suggested to range from 3:1 to 1:0 (Kok et al. 1970; Messinger and Renger 1993; Haumann and Junge 1994), which should not lead to a dip after J if the transition between S_1 and S_2 is fast enough. Therefore, a recorded dip in FI for dark-adapted leaves might indicate a decrease in the rate

Table 3 Comparisons of the major assumptions and results of current models of fluorescence induction

Model	Major assumptions	Major results and conclusions
Trissl and Lavergne (1995)	The model assumes (a) a homogeneous PSII population, (b) an exciton-radical pair equilibrium mechanism, (c) different rates of exciton transfer between core and peripheral antenna beds, (d) a calculation of fluorescence emission based on the amount of excited singlet chlorophyll in both core and peripheral antenna	A simple analytical relation is derived describing fluorescence induction kinetics under the presence of DCMU
Schreiber and Krieger (1996)	This model (a) assumes reversible radical pair mechanism, (b) assumes that Q_A reduction stimulates both prompt and recombinant fluorescence with only recombinant fluorescence being in competition with nonradiative energy losses at the reaction center, (c) does not include an oxygen evolution mechanism	Changes in the rate constants of nonradiative energy loss processes in PSII modulate the yield of recombination fluorescence in closed centers, which lead to fluorescence increase after J of FI. The fluorescence emission at the J phase can be purely attributed to prompt fluorescence with high enough rate constants of nonradiative energy loss processes in PSII
Stirbet et al. (1998)	The model incorporates reactions at both the acceptor side and the donor sides of photosystem II, and excitation energy quenching by the oxidized plastoquinone molecules from the lipid matrix of the thylakoid membrane. Chlorophyll fluorescence is calculated based on the redox state of Q_A	The point J corresponds to peak $[Q_A^-Q_B]$, the point I corresponds to peak $[Q_A^-Q_B^-]$, and point P corresponds to peak $[Q_A^-Q_B^-]$
Vredenberg (2000) (also see Vredenberg 2004)	The model (a) categorizes the reaction center into open, semi-open and closed states which can accept 2, 1 and 0 electrons respectively, (b) assumes that at least two turnovers are required for stationary closure of a reaction center, (c) considers the back transfer of excitons from open and semi-open reaction center to antenna	Light dependent changes in the rate constant of charge recombination causes changes in F_o . Fluorescence at point J corresponds to accumulation of photosynthetic units in the semi-open state. Fluorescence at point I is interpreted to be of systems with 100% of reaction centers closed
Lebedeva et al. (2002)	This model includes (a) a detailed description of reactions related to PSII, PSI, cyt b_6/f complex, ATP synthesis, and the possible leakage of H^+ , K^+ , and Cl^- through thylakoid membrane, (b) the dependence of electron transfer rate on the membrane potential, (c) no molecular mechanism of the oxygen evolution complex	The model describes FI under different light conditions. Fluorescence at every moment is determined by the sum of fluorescence emission by different fluorescence-emitting PSII states
Lazar (2003)	The model (a) assumes equilibrium of excited energy among all light harvesting and reaction center pigments, (b) assumes reversible radical pair formation mechanism, (c) considers both the acceptor side and donor side reactions and PSII heterogeneity, (d) calculates chlorophyll fluorescence based on concentrations of different forms of fluorescence-emitting excited state forms	(1) F_o phase is influenced by primary photochemistry of PSII and non-radiative loss of excitation energy, (2) the point J is influenced by P_{680}^+ quenching, changes in the rate constant of electron transfer from Q_A^- to Q_B due to different S states of OEC, (3) the P point is influenced by the state transition of OEC and electron transfer from Q_A^- to Q_B
Our model	Our model (a) assumes a reversible radical pair model, (b) describes the energy transfer between different antenna components, (c) considers both the acceptor and donor side electron transfer reactions, (d) calculates fluorescence emission based on the amount of excited singlet-state chlorophylls, (e) considers the Q_B^- -reducing and Q_B^- -nonreducing PSII centers	The point J corresponds to the peak $[Q_A^-Q_B^-]$ and $[Q_A^-Q_B]$. The point I corresponds to the first shoulder of the $[Q_A^-Q_B^-]$. The P point corresponds to the peak $[Q_A^-Q_B^-]$ and $[PQH_2]$. The dip after J phase is closely associated with P_{680}^+ quenching. The relative size of core antenna and peripheral antenna influences the F_o level

constant of the transition between S_1 and S_2 states in the OEC, or a decrease in the ratio of $S_1:S_0$, which causes transient accumulation of P_{680}^+ .

Changing the $Q_B:Q_B^-$ ratio influences the appearance of point J in FI. As shown in Fig. 4b, the fluorescence emission at the point J gradually increases and finally reaches the fluorescence emission of point I when the initial state of $Q_B:Q_B^-$ is changed from 1:0 to 0:1 (Fig. 6d). Therefore, the relative redox state of Q_B appears to determine the fluorescence emission at point J relative to point I in FI. A $Q_B:Q_B^-$ of 0.5:0.5 is consistent with that reported for dark-adapted leaves (Rutherford et al. 1984).

The fluorescence emission at point P is influenced by both the rate constant of plastoquinone oxidation (k_{ox}) (Fig. 5e) and the PQ pool size (Fig. 5f). Fluorescence at P reflects a balance between light incident at the PSII side and the rate of utilization of the chemical (potential) energy and the rate of heat dissipation. In our model, PQH_2 oxidation by the cytochrome b_6f complex (with a rate constant k_{ox}) represents the final fate of the chemical energy. Higher k_{ox} leads to a higher rate of energy utilization, which indirectly decreases the amount of excitation energy available for dissipation as fluorescence since more energy can be utilized in photochemistry. Furthermore, higher k_{ox} increases the oxidation state of PQ at steady state under a given light flux. Higher oxidized PQ concentration quenches excitation energy and therefore lowers fluorescence emission (Vernotte et al. 1979) (Fig. 5e). Therefore, changes in the fluorescence emission at P for a leaf sample under certain treatment can be used to monitor the changes in PQH_2 oxidation. Changes in the PQ pool size change fluorescence emission at P (Fig. 5f). Increases in the PQ pool size in the thylakoid membrane leads to a higher oxidized PQ concentration, which results in decreased fluorescence emission at P (Fig. 5f).

Finally, increasing the proportion of Q_B -nonreducing PSII centers decreased F_v/F_m (Fig. 7). In this model, with increase in the proportion of Q_B -nonreducing PSII centers, more incident excitation energy is absorbed by the core antennae of Q_B -nonreducing PSII centers and chlorophylls in peripheral antennae detached from the Q_B -nonreducing center. Our model assumes that excitation energy incident on chlorophylls detached from Q_B -nonreducing PSII center dissipates only in the form of either heat or fluorescence, and it does not transfer to Q_B -reducing PSII reaction centers for charge separation. Therefore, with increase in Q_B -nonreducing center, a higher proportion of the incident energy is diverted into fluorescence and heat dissipation rather than being utilized in primary charge separation. As a result, increase in the proportion of Q_B -nonreducing PSII centers increases fluorescence emission at the O phase (Fig. 7), which leads to a linear decrease in F_v/F_m . This may explain systematic differences in F_v/F_m observed between taxonomic groups in the absence of photoinhibition (Long et al. 1993).

Acknowledgements This work was co-supported by the National Center for Supercomputing Applications, and the U. S. National Science Foundation IBN 04-17126. We thank Reto J. Strasser and D. Lazar for corrections in the proofs.

Appendix 1

The ordinary differential equations representing the model of fluorescence induction (Fig. 1). This set of equations only includes the differential equations representing the change of concentrations of components associated with Q_B -reducing PSII reaction centers. Same set of different equations were used to describe the concentration changes of components associated with Q_B -nonreducing PSII reaction centers. The Q_B -nonreducing and Q_B -reducing reaction centers were assumed to share the same plastoquinol pool. The differential equation for $[PQH_2]$ in the full model combines the contributions from reactions associated with both Q_B -reducing and Q_B -nonreducing reaction centers. The rate equation for each velocity variable is listed in Appendix 2. The abbreviations of reaction velocities used in the system of differential equations are defined in Appendix 3.

$$\begin{aligned} \frac{d[A_p]}{dt} &= I_a - v_{Af} - v_{Ad} - v_{AU} + v_{UA} \\ &\quad - v_{P680qA} - v_{PQqA} \end{aligned}$$

$$\begin{aligned} \frac{d[U]}{dt} &= I_c + v_{AU} - v_{UA} - v_{Uf} - v_{Ud} \\ &\quad - v_{P680qU} - v_1 + v_{-1} - v_{PQqU} \end{aligned}$$

$$\frac{d[P_{680}^+P_{heo}^-]}{dt} = v_1 - v_{-1} - v_{z-1} - v_{z-2} + v_{r2-1}$$

$$\frac{d[P_{680}^+P_{heo}]}{dt} = v_{z-1} - v_{r2-1} - v_{z-2}$$

$$\frac{d[P_{680}P_{heo}^-]}{dt} = v_{z-1} - v_{z-2} + v_{r2-2}$$

$$\frac{d[S_{1T}]}{dt} = v_{s0-s1} - v_{1Z}$$

$$\frac{d[S_{2T}]}{dt} = v_{s1-s2} - v_{2Z}$$

$$\frac{d[S_{3T}]}{dt} = v_{s2-s3} - v_{3Z}$$

$$\frac{d[S_{0T}]}{dt} = v_{s3-s0} - v_{0Z}$$

$$\frac{d[S_{1Tp}]}{dt} = v_{1Z} - v_{s1-s2}$$

$$\frac{d[S_{2Tp}]}{dt} = v_{2Z} - v_{s2-s3}$$

$$\frac{d[S_{3Tp}]}{dt} = v_{3Z} - v_{s3-s0}$$

$$\frac{d[S_{0Tp}]}{dt} = v_{0Z} - v_{s0-s1}$$

$$\frac{d[Q_A Q_B]}{dt} = v_3 - v_{J3} - v_{2,00,1} - v_{2,00,2} + v_{r2,00,1} + v_{r2,00,2}$$

$$\begin{aligned} \frac{d[Q_A^- Q_B]}{dt} &= v_{2,00,1} + v_{2,00,2} - v_{r2,00,1} - v_{r2,00,2} - v_{AB1} \\ &\quad + v_{BA1} + v_{3,J1} - v_{J3,J1} \end{aligned}$$

$$\frac{d[Q_A Q_B^-]}{dt} = v_{AB1} - v_{BA1} - v_{2,01,1} - v_{2,01,2} + v_{r2,01,1} + v_{r2,01,2}$$

$$\frac{d[Q_A^- Q_B^-]}{dt} = v_{BA2} - v_{AB2} + v_{2,01,1} + v_{2,01,2} - v_{r2,01,1} - v_{r2,01,2}$$

$$\begin{aligned} \frac{d[Q_A Q_B^2]}{dt} &= v_{AB2} - v_{BA2} - v_3 + v_{J3} - v_{2,02,1} \\ &\quad - v_{2,02,2} + v_{r2,02,1} + v_{r2,02,2} \end{aligned}$$

$$\frac{d[Q_A^- Q_B^2]}{dt} = v_{J3,J1} - v_{3,J1} + v_{2,02,1} + v_{2,02,2} - v_{r2,02,1} - v_{r2,02,2}$$

$$\frac{d[PQH_2]}{dt} = v_3 + v_{3,J1} - v_{J3} - v_{J3,J1} - v_{pq-ox}$$

Appendix 2

The rate equations describing the reactions associated with Q_B -reducing reaction centers used in the model of fluorescence induction. The set of equations for the reactions associated with the Q_B -nonreducing reaction centers were similar to this set and not listed. See Appendix 3 for definition of abbreviations. The details for derivation of each rate equations are in the main text. The detailed description for each abbreviation is listed in Appendix 3 except that the rate constants are listed in Table 1.

$$I_a = \frac{220I_m}{(290+200n)(1+x)}$$

$$I_c = \frac{70I_m}{(290+200n)(1+x)}$$

$$A_i = \frac{220xI_m}{(290+200n)(1+x)}$$

$$U_{if} = \frac{35xI_m}{(290+200n)(1+x)}$$

$$v_{Af} = [A_p]k_f^a$$

$$v_{Ad} = [A_p]k_d^a$$

$$v_{AU} = [A_p]k_{AU} \left(\frac{1-x}{1+x} \right)$$

$$v_{UA} = [U]k_{UA}$$

$$v_{Uf} = [U]k_f^u$$

$$v_{Ud} = [U](1-q)k_d^{Uc} + [U]qk_d^{Uo}$$

$$\text{where } q = [Q_A]/([Q_A] + [Q_A^-])$$

$$\text{where } [Q_A] = [Q_A Q_B] + [Q_A Q_B^-] + [Q_A Q_B^{2-}]$$

$$[Q_A^-] = [Q_A^- Q_B] + [Q_A^- Q_B^-] + [Q_A^- Q_B^{2-}]$$

$$v_1 = q[P_{680}^* \text{Pheo}]k_1^o + [P_{680}^* \text{Pheo}](1-q) \times (1-p)k_1^c + [P_{680}^* \text{Pheo}](1-q)pk_1^o \quad \text{where}$$

$$[P_{680}^* \text{Pheo}] = [U][P_{680} \text{Pheo}](1 + \frac{k_{-t}}{k_t})^{-1} / 70$$

$$\text{and } \frac{k_{-t}}{k_t} = \exp[-hc/(kT)(\lambda_{Chl}^{-1} - \lambda_p^{-1})]$$

$$v_{-1} = q[P_{680}^+ \text{Pheo}^-]k_{-1}^o + (1-q)[P_{680}^+ \text{Pheo}^-]k_{-1}^c$$

$$v_{S1_S2} = [S_{1Tp}]k_{o12}$$

$$v_{S2_S3} = [S_{2Tp}]k_{o23}$$

$$v_{S3_S0} = [S_{3Tp}]k_{o30}$$

$$v_{S0_S1} = [S_{0Tp}]k_{o01}$$

$$\text{Coeff1} = \frac{[P_{680}^+ \text{Pheo}^-]}{[P_{680} \text{PheoT}]}$$

$$\text{where } [P_{680} \text{PheoT}] = [P_{680} \text{Pheo}] + [P_{680}^+ \text{Pheo}] + [P_{680} \text{Pheo}^-] + [P_{680}^+ \text{Pheo}^-]$$

$$v_{1z_1} = [S_{1T}]k_z \text{Coeff1}$$

$$v_{2z_1} = [S_{2T}]k_z \text{Coeff1}$$

$$v_{3z_1} = [S_{3T}]k_z \text{Coeff1}$$

$$v_{0z_1} = [S_{0T}]k_z \text{Coeff1}$$

$$v_{z_1} = v_{1z_1} + v_{2z_1} + v_{3z_1} + v_{0z_1}$$

$$\text{Coeff2} = \frac{[P_{680}^+ \text{Pheo}]}{[P_{680} \text{PheoT}]}$$

$$v_{1z_2} = [S_{1T}]k_z \text{Coeff2}$$

$$v_{2z_2} = [S_{2T}]k_z \text{Coeff2}$$

$$v_{3z_2} = [S_{3T}]k_z \text{Coeff2}$$

$$v_{0z_2} = [S_{0T}]k_z \text{Coeff2}$$

$$v_{z_2} = v_{1z_2} + v_{2z_2} + v_{3z_2} + v_{0z_2}$$

$$v_{1z} = v_{1z_1} + v_{1z_2}$$

$$v_{2z} = v_{2z_1} + v_{2z_2}$$

$$v_{3z} = v_{3z_1} + v_{3z_2}$$

$$v_{0z} = v_{0z_1} + v_{0z_2}$$

$$v_{AB1} = [Q_A^- Q_B]k_{AB1}$$

$$v_{BA1} = [Q_A Q_B^-]k_{BA1}$$

$$v_{AB2} = [Q_A^- Q_B^-]k_{AB2}$$

$$v_{BA2} = [Q_A Q_B^{2-}]k_{BA2}$$

$$[PQT] = 6$$

$$v_3 = [Q_A Q_B^{2-}]k_3[PQ]/[PQT]$$

$$v_{-r3} = [Q_A Q_B]k_{r3}[PQH_2]/[PQT]$$

$$v_{3_n} = [Q_A^- Q_B^{2-}]k_3[PQ]/[PQT]$$

$$v_{-r3_n} = [Q_A^- Q_B]k_{r3}[PQH_2]/[PQT]$$

$$v_{-pq_ox} = [PQH_2]k_{ox}$$

$$v_{2_1} = [P_{680}^+ \text{Pheo}^-]k_2q$$

$$v_{2_2} = [P_{680} \text{Pheo}^-]k_2q$$

$$a = [Q_A Q_B]/([Q_A Q_B] + [Q_A Q_B^-] + [Q_A Q_B^{2-}])$$

$$b = [Q_A Q_B^-]/([Q_A Q_B] + [Q_A Q_B^-] + [Q_A Q_B^{2-}])$$

$$c = [Q_A Q_B^{2-}]/([Q_A Q_B] + [Q_A Q_B^-] + [Q_A Q_B^{2-}])$$

$$v_{2_00_1} = v_{2_1}a$$

$$v_{2_01_1} = v_{2_1}b$$

$$v_{2_02_1} = v_{2_1}c$$

$$v_{2_00_2} = v_{2_2}a$$

$$v_{2_01_2} = v_{2_2}b$$

$$v_{2_02_2} = v_{2_2}c$$

$$CE_1 = \frac{[P_{680}^+ \text{Pheo}]}{[P_{680} \text{PheoT}]}$$

$$v_{r2_00_1} = CE_1[Q_A^- Q_B]k_2/Ke$$

$$v_{r2_01_1} = CE_1[Q_A^- Q_B^-]k_2/Ke$$

$$v_{r2_02_1} = CE_1[Q_A^- Q_B^{2-}]k_2/Ke$$

$$v_{r2_1} = v_{r2_00_1} + v_{r2_01_1} + v_{r2_02_1}$$

$$CE_2 = \frac{[P_{680} \text{Pheo}]}{[P_{680} \text{PheoT}]}$$

$$v_{r2_00_2} = CE_2[Q_A^- Q_B]k_2/Ke$$

$$v_{r2_01_2} = CE_2[Q_A^- Q_B^-]k_2/Ke$$

$$v_{r2_02_2} = CE_2[Q_A^- Q_B^{2-}]k_2/Ke$$

$$v_{r2_2} = v_{r2_00_2} + v_{r2_01_2} + v_{r2_02_2}$$

$$v_{P680qU} = [U]([P_{680}^+ \text{Pheo}] + [P_{680} \text{Pheo}^-])k_c$$

$$v_{P680qA} = [A]([P_{680}^+ \text{Pheo}] + [P_{680} \text{Pheo}^-])k_c$$

$$k_q = 0.15(k_f + k_h)/[PQT]$$

$$v_{PQqU} = [U][PQ]k_q$$

$$v_{PQqA} = [A][PQ]k_q$$

$$F = k_f^a A_p + ([U] + [U_i])k_f^u + k_f^a [A_{ip}] + k_f^u [U_{ifc}]$$

Appendix 3

Definitions of all abbreviations except rate constants used in the model

Abbrev.	Description	Unit
$[A_p]$	Concentration of excitation energy on peripheral antenna of photosystem II	$\mu\text{mol m}^{-2}$
$[P_{680}^+ \text{Pheo}]$	The concentration of excited P_{680} associated with Pheo	$\mu\text{mol m}^{-2}$
$[P_{680}^+ \text{Pheo}]$	The concentration of P_{680}^+ associated with Pheo	$\mu\text{mol m}^{-2}$
$[P_{680}^+ \text{Pheo}^-]$	The concentration of P_{680}^+ associated with Pheo^-	$\mu\text{mol m}^{-2}$
$[P_{680} \text{Pheo}]$	The concentration of P_{680} associated with Pheo	$\mu\text{mol m}^{-2}$
$[P_{680} \text{Pheo}^-]$	The concentration of P_{680} associated with Pheo^-	$\mu\text{mol m}^{-2}$
$[P_{680} \text{PheoT}]$	The total concentration of $P_{680} \text{Pheo}$, $P_{680}^+ \text{Pheo}$, $P_{680} \text{Pheo}^-$ and $P_{680}^+ \text{Pheo}^-$.	$\mu\text{mol m}^{-2}$
$[PQ]$	The concentration of oxidized plastoquinone	$\mu\text{mol m}^{-2}$
$[PQH_2]$	The concentration of fully reduced plastoquinone	$\mu\text{mol m}^{-2}$
$[PQT]$	The total concentration of plastoquinone and plastoquinol in thylakoid membrane	$\mu\text{mol m}^{-2}$
$[Q_A]$	The concentration of oxidized Q_A	$\mu\text{mol m}^{-2}$
$[Q_A^-]$	The concentration of reduced Q_A	$\mu\text{mol m}^{-2}$
$[Q_A Q_B]$	The concentration of oxidized Q_A associated with oxidized Q_B	$\mu\text{mol m}^{-2}$
$[Q_A^- Q_B]$	The concentration of reduced Q_A associated with oxidized Q_B	$\mu\text{mol m}^{-2}$
$[Q_A^- Q_B^-]$	The concentration of reduced Q_A associated with Q_B^-	$\mu\text{mol m}^{-2}$
$[Q_A Q_B^-]$	The concentration of reduced Q_A associated with Q_B^-	$\mu\text{mol m}^{-2}$
$[Q_A Q_B^{\cdot-}]$	The concentration of oxidized Q_A associated with $Q_B^{\cdot-}$	$\mu\text{mol m}^{-2}$
$[Q_A Q_B^{\cdot-}]$	The concentration of oxidized Q_A associated with $Q_B^{\cdot-}$	$\mu\text{mol m}^{-2}$
$[S_n]$	The concentration of oxygen evolving complex at S_n state	$\mu\text{mol m}^{-2}$
$[S_{nT}]$	The concentration of oxygen evolving complex at S_n state before donating electron to tyrosine (Y_2)	$\mu\text{mol m}^{-2}$
$[S_{nTp}]$	The concentration of oxygen evolving complex at S_n state after donating electron to tyrosine (Y_2)	$\mu\text{mol m}^{-2}$
$[U]$	Concentration of excitation energy on core antenna of Q_B -reducing photosystem II	$\mu\text{mol m}^{-2}$
$[U_i]$	Concentration of excitation energy on core antenna of Q_B -nonreducing photosystem II	$\mu\text{mol m}^{-2}$
$[U_{ifc}]$	The concentration of excitation energy on chlorophylls detached from core antenna of Q_B -nonreducing photosystem II	$\mu\text{mol m}^{-2}$
$[Y_Z]$	The concentration of primary electron donor for reaction center of PSII (P_{680})	$\mu\text{mol m}^{-2}$
A_i	Incident photon flux density on peripheral antenna of Q_B -nonreducing photosystem II	$\mu\text{mol m}^{-2} \text{ s}^{-1}$
A_{iP}	The concentration of excitation energy on peripheral antenna of Q_B -nonreducing photosystem II	$\mu\text{mol m}^{-2}$
I_A	The incident photon flux density on peripheral PSII antenna	$\mu\text{mol m}^{-2} \text{ s}^{-1}$
I_c	The incident photon flux density on core antenna of Q_B -reducing reaction center	$\mu\text{mol m}^{-2} \text{ s}^{-1}$
I_{in}	The total incident photon flux density	$\mu\text{mol m}^{-2} \text{ s}^{-1}$
n	The ratio of PSI to PSII	NA
P_{680}	The reaction center chlorophyll of PSII. It can exist in native state (P_{680}), excited state (P_{680}^*), or oxidized state (P_{680}^+).	NA
Pheo	Pheophytin, the first electron acceptor of primary charge separation in PSII. It can exist in either native state (Pheo) or reduced state (Pheo^-).	NA
q	The proportion of oxidized Q_A	NA
Q_A	The first quinone electron acceptor of PSII	NA
Q_B	The second quinone electron acceptor of PSII	NA
U_{if}	Incident photon flux density on chlorophylls detached from core antenna of Q_B -nonreducing photosystem II	$\mu\text{mol m}^{-2} \text{ s}^{-1}$
v_{pq_ox}	The rate of PQH_2 oxidation by Cyt b_6f	$\mu\text{mol m}^{-2} \text{ s}^{-1}$
v_{r3}	The rate of the exchange of PQH_2 with Q_B associated with Q_A	$\mu\text{mol m}^{-2} \text{ s}^{-1}$
v_{r3_n}	The rate of exchange of PQH_2 with Q_B associated with Q_A^-	$\mu\text{mol m}^{-2} \text{ s}^{-1}$
v_1	The rate of charge separation in the Q_B -reducing PSII reaction center	$\mu\text{mol m}^{-2} \text{ s}^{-1}$
v_{-1}	The rate of charge recombination in the Q_B -reducing PSII reaction center	$\mu\text{mol m}^{-2} \text{ s}^{-1}$
$v_{2_0m_n}$	The rate of reactions relating to electron transfer from Pheo^- to Q_A where m represents the redox state of Q_B with 0 for Q_B , 1 for Q_B^- and 2 for $Q_B^{\cdot-}$, and n represents the redox state of P_{680} with 1 for P_{680}^+ and 2 for P_{680} , e.g. $v_{2_00_1}$: the rate of reduction of $Q_A Q_B$ by $P_{680}^+ \text{Pheo}^-$	$\mu\text{mol m}^{-2} \text{ s}^{-1}$
v_{2_1}	The rate of Q_A reduction by $P_{680}^+ \text{Pheo}^-$	$\mu\text{mol m}^{-2} \text{ s}^{-1}$
v_{2_2}	The rate of Q_A reduction by $P_{680} \text{Pheo}^-$	$\mu\text{mol m}^{-2} \text{ s}^{-1}$
v_3	The rate of exchange of PQ with $Q_B^{\cdot-}$ associated with Q_A	$\mu\text{mol m}^{-2} \text{ s}^{-1}$
v_{3_n}	The rate of exchange of PQ with $Q_B^{\cdot-}$ associated with Q_A^-	$\mu\text{mol m}^{-2} \text{ s}^{-1}$
v_{AB1}	The rate of electron transfer from Q_A^- to Q_B	$\mu\text{mol m}^{-2} \text{ s}^{-1}$

Abbrev.	Description	Unit
v_{AB2}	The rate of electron transfer from Q_A^- to Q_B^-	$\mu\text{mol m}^{-2} \text{s}^{-1}$
v_{Ad}	The rate of heat dissipation from the peripheral antenna	$\mu\text{mol m}^{-2} \text{s}^{-1}$
v_{Af}	The rate of fluorescence emission from the peripheral antenna	$\mu\text{mol m}^{-2} \text{s}^{-1}$
v_{AU}	The rate of excitation energy transfer from peripheral to core antenna	$\mu\text{mol m}^{-2} \text{s}^{-1}$
v_{BA1}	The rate of electron transfer from Q_B^- to Q_A	$\mu\text{mol m}^{-2} \text{s}^{-1}$
v_{BA2}	The rate of electron transfer from Q_B^- to Q_A	$\mu\text{mol m}^{-2} \text{s}^{-1}$
v_{nz}	The rate of oxidation of S_n state of oxygen evolution complex	$\mu\text{mol m}^{-2} \text{s}^{-1}$
v_{nz_1}	The rate of electron transfer from oxygen evolution complex at S_n state to P_{680}^+ associated with Pheo ⁻ via Y_z	$\mu\text{mol m}^{-2} \text{s}^{-1}$
v_{nz_2}	The rate of electron transfer from oxygen evolution complex at S_n state to P_{680}^+ associated with Pheo via Y_z	$\mu\text{mol m}^{-2} \text{s}^{-1}$
v_{P680qA}	The rate of quenching of excitation energy in the peripheral antenna by P_{680}^+	$\mu\text{mol m}^{-2} \text{s}^{-1}$
v_{P680qU}	The rate of quenching of excitation energy in the core antenna by P_{680}^+	$\mu\text{mol m}^{-2} \text{s}^{-1}$
v_{PQqA}	The rate of quenching of excitation energy in the peripheral antenna by oxidized plastoquinone	$\mu\text{mol m}^{-2} \text{s}^{-1}$
v_{PQqU}	The rate of quenching of excitation energy in the core antenna by oxidized plastoquinone	$\mu\text{mol m}^{-2} \text{s}^{-1}$
$v_{r2_0m_n}$	The back reaction of $v_{2_0m_n}$, see $v_{2_0m_n}$ for details	$\mu\text{mol m}^{-2} \text{s}^{-1}$
v_{r2_1}	The rate of Q_A^- oxidation by P_{680}^+ Pheo	$\mu\text{mol m}^{-2} \text{s}^{-1}$
v_{r2_2}	The rate of Q_A^- oxidation by P_{680}^+ Pheo	$\mu\text{mol m}^{-2} \text{s}^{-1}$
v_{sm_sn}	The rate of transition from S_m state to S_n state of oxygen evolution complex	$\mu\text{mol m}^{-2} \text{s}^{-1}$
v_{UA}	The rate of excitation energy transfer from core antenna to peripheral antenna	$\mu\text{mol m}^{-2} \text{s}^{-1}$
v_{Ud}	The rate of heat dissipation of excitation energy from the core antenna of Q_B^- -reducing PSII reaction center	$\mu\text{mol m}^{-2} \text{s}^{-1}$
v_{Uf}	The rate of fluorescence emission from the core antenna of Q_B^- -reducing reaction center	$\mu\text{mol m}^{-2} \text{s}^{-1}$
v_{z_1}	The rate of P_{680}^+ Pheo ⁻ reduction	$\mu\text{mol m}^{-2} \text{s}^{-1}$
v_{z_2}	The rate of P_{680}^+ Pheo reduction	$\mu\text{mol m}^{-2} \text{s}^{-1}$
x	The ratio of the concentration of Q_B^- -nonreducing PSII reaction center to that of Q_B^- -reducing reaction center	NA
F	Total fluorescence intensity	$\mu\text{mol m}^{-2} \text{s}^{-1}$

References

- Baake E, Schloder JP (1992) Modeling the fast fluorescence rise of photosynthesis. *Bull Math Biol* 54:999–1021
- Baker NR, Oxborough K (2004) Chlorophyll fluorescence as a probe of photosynthetic productivity. In: Papageorgiou GC, Govindjee (eds) *Chlorophyll a fluorescence: a signature of photosynthesis*. Springer, Dordrecht, pp 65–82
- Baker NR, East TM, Long SP (1983) Chilling damage to photosynthesis in young *Zea mays*. *J Exp Bot* 34:189–197
- Ben-Shem A, Frolov F, Nelson N (2003) Crystal structure of plant photosystem I. *Nature* 426:630–635
- Bolhár-Nordenkamp HR, Long SP, Baker NR, Qquist G, Schreiber U, Lechner EG (1989) Chlorophyll fluorescence as a probe of the photosynthetic competence of leaves in the field—a review of current instrumentation. *Funct Ecol* 3:497–514
- Bouges Bocquet B (1977) Cytochrome f and plastocyanin kinetics in *C. pyrenoidosa*. *Biochim Biophys Acta* 462:362–370
- Bowes J, Crofts AR (1980) Binary oscillations in the rate of reoxidation of the primary acceptor of photosystem II. *Biochim Biophys Acta* 590:373–384
- Bowes J, Crofts AR, Arntzen CJ (1980) Redox reactions on the reducing side of photosystem-II in chloroplasts with altered herbicide binding-properties. *Arch Biochem Biophys* 200:303–308
- Brettel K, Schlodder E, Witt HT (1984) Nanosecond reduction kinetics of photooxidized chlorophyll a_{11} (P-680) in single flashes as a probe for the electron pathway, H^+ -release and charge accumulation in the O_2 -evolving complex. *Biochim Biophys Acta* 766:403–415
- Brody SS (2002) Fluorescence lifetime, yield, energy transfer and spectrum in photosynthesis, 1950–1960. *Photosynth Res* 73:127–132
- Butler WL (1972) On the primary nature of fluorescence yield changes associated with photosynthesis. *P Natl Acad Sci USA* 69:3420–3422
- Chitnis PR (2001) Photosystem I: function and physiology. *Annu Rev Plant Physiol Plant Mol Biol* 52:593–636
- Chylla RA, Whitmarsh J (1990) Light saturation response of inactive photosystem-II reaction centers in spinach. *Photosynth Res* 25:39–48
- Crofts AR, Robinson HH, Snozzi M (1984) Reactions of quinones at catalytic sites: a diffusional role in H^+ transfer. In Sybesma C (ed) *Advances in photosynthesis research*. volume 1. Martinus Nijhoff/Dr W Junk Publishers, The Hague, Netherlands, pp 461–468
- Crofts AR, Baroli I, Kramer D, Taoka S (1993) Kinetics of electron-transfer between Q_A and Q_B in wild-type and herbicide-resistant mutants of *Chlamydomonas reinhardtii*. *Z Naturforsch C-a J Biosci* 48:259–266
- Dau H (1994) Molecular mechanisms and quantitative models of variable photosystem II fluorescence. *Photochem Photobiol* 60:1–23
- Dekker JP, Plijter JJ, Ouwehand L, van Gorkom HJ (1984) Kinetics of manganese redox transitions in the oxygen evolving complex of photosystem II. *Biochim Biophys Acta* 767:176–179
- Delosme R (1967) Etude de l'induction de fluorescence des algues vertes et des chloroplastes au debut d'une illumination intense. *Biochim Biophys Acta* 143:108–128
- Delosme R (1971) New results about chlorophyll fluorescence in vivo. In: Forti G, Avron M, Melandri A (eds) *Proceedings of the 11th international congress on photosynthesis research*. volume 1. Martinus Nijhoff/Dr W Junk, The Hague, Netherlands, pp 187–95
- Deprez J, Paillot G, Dobek A, Leibl W, Trissl HW, Breton J (1990) Competition between energy trapping and exciton annihilation in the lake model of the photosynthetic membrane of purple bacteria. *Biochim Biophys Acta* 1015:295–303
- Diner BA (1977) Dependence of deactivation reactions of photosystem II on the redox state of the plastoquinone pool A, varied under anaerobic conditions. Equilibria on the acceptor side of photosystem II. *Biochim Biophys Acta* 460:247–258
- Ferreira KN, Iverson TM, Maghlaoui K, Barber J, Iwata S (2004) Architecture of the photosynthetic oxygen-evolving center. *Science* 303:1831–1838
- Forbush B, Kok B, McGloin MP (1971) Cooperation of charges in photosynthetic O_2 evolution. II. Damping of flash yield oscillation and deactivation. *Photochem Photobiol* 14:307–321
- Golbeck JH, Kok B (1979) Redox titration of electron acceptor Q and the plastoquinone pool in photosystem II. *Biochim Biophys Acta* 547:347–360
- Govindjee (1995) Sixty -three years since Kautsky: chlorophyll a fluorescence. *Aust J Plant Physiol* 22:131–160

- Govindjee (2004) Chlorophyll fluorescence: a bit of basics and history. In: Papageorgiou GC, Govindjee (eds) Chlorophyll *a* fluorescence: a signature of photosynthesis. Springer, Dordrecht, pp 1–42
- van Grondelle R, Gobets B (2004) Transfer and trapping of excitation in plant photosystems. In: Papageorgiou C, Govindjee (eds) Chlorophyll fluorescence: a signature of photosynthesis. Springer, Dordrecht, pp 107–132
- Guenther JE, Melis A (1990) The physiological significance of photosystem-II heterogeneity in chloroplasts. *Photosynth Res* 23:105–109
- Haehnel W (1976) The reduction kinetics of chlorophyll *a* 1 as indicator for proton uptake between light reactions in chloroplasts. *Biochim Biophys Acta* 440:506–521
- Hankamer B, Barber J, Boekema EJ (1997) Structure and membrane organization of photosystem II in green plants. *Annu Rev Plant Physiol Plant Mol Biol* 48:641–671
- Haumann M, Junge W (1994) Extent and rate of proton release by photosynthetic water oxidation in thylakoids: electrostatic relaxation versus chemical production. *Biochemistry* 33:864–872
- Haumann M, Junge W (1994) The rates of proton uptake and electron-transfer at the reducing side of photosystem-II in thylakoids. *FEBS Lett* 347:45–50
- Horton P, Ruban AV, Walters RG (1996) Regulation of light harvesting in green plants. *Annu Rev Plant Physiol Plant Mol Biol* 47:655–684
- Joliot A, Joliot P (1964) Etude cinétique de la réaction photochimique libérant l'oxygène au cours de la photosynthèse. *Comput Rend Acad Sci Paris* 258:4622–4625
- Joliot P, Joliot A (2003) Excitation transfer between photosynthetic units: the 1964 experiment. *Photosynth Res* 76:241–245
- Joliot P, Lavergne J, Beal D (1992) Plastoquinone compartmentation in chloroplasts. I Evidence for domains with different rates of photo-reduction. *Biochim Biophys Acta* 1101:1–12
- Kok B, Forbush B, McGloin MP (1970) Cooperation of charges in photosynthetic O₂ evolution I A linear four step mechanism. *Photochem Photobiol* 11:457–475
- Kramer DM, Dimarco G, Loreto F (1995) Contribution of plastoquinone quenching to saturation pulse-induced rise of chlorophyll fluorescence in leaves. In Mathis P (ed) Photosynthesis from light to the biosphere. volume 1. Kluwer, Dordrecht, pp 147–150
- Krause GH, Weis E (1991) Chlorophyll fluorescence and photosynthesis-the basics. *Annu Rev Plant Physiol Plant Mol Biol* 42:313–349
- Laible P, Zipfel W, Owens T (1994) Excited state dynamics in chlorophyll based antennae: the rate of transfer equilibrium. *Biophys J* 66:844–860
- Lavergne J, Briantais JM (1996) Photosystem-II heterogeneity. In: Ort DR, Yocum CF (eds) Oxygen photosynthesis: the light reactions. Kluwer, Dordrecht, pp 265–287
- Lavergne J, Trissl HW (1995) Theory of fluorescence induction in photosystem II - derivation of analytical expressions in a model including exciton-radical- pair equilibrium and restricted energy transfer between photosynthetic units. *Biophys J* 68:2474–2492
- Lazar D (1999) Chlorophyll *a* fluorescence induction. *Biochim Biophys Acta* 1412:1–28
- Lazar D (2003) Chlorophyll *a* fluorescence rise induced by high light illumination of dark-adapted plant tissue studied by means of a model of photosystem II and considering photosystem II heterogeneity. *J Theor Biol* 220:469–503
- Lazar D, Pospisil P (1999) Mathematical simulation of chlorophyll *a* fluorescence rise measured with 3-(3', 4'-dichlorophenyl)-1,1-dimethylurea barley leaves at room and high temperatures. *Eur Biophys J* 28:468–477
- Lazar D, Naus J, Matouskova M, Flasarova M (1997) Mathematical modeling of changes in chlorophyll fluorescence induction caused by herbicides. *Pestic Biochem Physiol* 57:200–210
- Lazar D, Brokes M, Naus J, Dvorak L (1998) Mathematical modelling of 3-(3', 4'-dichlorophenyl)-1,1-dimethylurea action in plant leaves. *J Theor Biol* 191:79–86
- Lebedeva GV, Belyaeva NE, Demin OV, Riznichenko GY, Rubin AB (2002) Kinetic model of primary photosynthetic processes in chloroplasts description of the fast phase of chlorophyll fluorescence induction under different light intensities. *Biophysics* 47:968–980
- Liu ZF, Yan HC, Wang KB, Kuang TY, Zhang JP, Gui LL, An XM, Chang WR (2004) Crystal structure of spinach major light-harvesting complex at 2.72 angstrom resolution. *Nature* 428:287–292
- Long SP, Postl WF, Bolhár-Nordenkampf HR (1993) Quantum yields for uptake of carbon dioxide in C3 vascular plants of contrasting habitats and taxonomic groupings. *Planta* 189:226–234
- Long SP, Humphries SW, Falkowski PG (1994) Photoinhibition of photosynthesis in nature. *Ann Rev Plant Physiol Mol Biol* 45:633–662
- Melis A (1991) Dynamics of photosynthetic membrane-composition and function. *Biochim Biophys Acta* 1058:87–106
- Messinger J, Renger G (1993) Generation, oxidation by the oxidized form of the tyrosine of polypeptide D2, and possible electronic configuration of the redox states S₀, S₁ and S₂ of the water oxidase in isolated spinach thylakoids. *Biochemistry* 32:9379–9386
- Meunier PC (1993) Oxygen evolution by photosystem II - the contribution of backward transitions to the anomalous behavior of double-hits revealed by a new analysis method. *Photosynth Res* 36:111–118
- Meunier PC, Burnap RL, Sherman LA (1996) Improved 5-step modeling of the Photosystem II S-state mechanism in cyanobacteria. *Photosynth Res* 47:61–76
- Meyer B, Schlodder E, Dekker JP, Witt HT (1989) O₂ evolution and Chl *a* II⁺ (P₆₈₀⁺) nanosecond reduction kinetics in single flashes as a function of pH. *Biochim Biophys Acta* 974:36–43
- Mitchell R, Spillmann A, Haehnel W (1990) Plastoquinol diffusion in linear photosynthetic electron-transport. *Biophys J* 58:1011–1024
- Neubauer C, Schreiber U (1987) The polyphasic rise of chlorophyll fluorescence upon onset of strong continuous illumination: I Saturation characteristics and partial control by photosystem II acceptor side. *Zeitschrift für Naturforschung* 42c:1426–1254
- Niyogi KK (1999) Photoprotection revisited: genetic and molecular approaches. *Annu Rev Plant Physiol Plant Mol Biol* 50:333–359
- Packham NK, Hodges M, Etienne AL, Briantais JM (1988) Changes in the flash-induced oxygen yield pattern by thylakoid membrane phosphorylation. *Photosynth Res* 15:221–232
- Peter GF, Thornber JP (1991) Biochemical composition and organization of higher plant photosystem II light harvesting pigment proteins. *J Biol Chem* 266:16745–16754
- Quigg A, Beardall J, Wydrzynski T (2003) Photoacclimation involves modulation of the photosynthetic oxygen-evolving reactions in *Dunaliella tertiolecta* and *Phaeodactylum tricoratum*. *Funct Plant Biol* 30:301–308
- Robinson HH, Crofts AR (1983) Kinetics of the oxidation-reduction reactions of the photosystem II quinone acceptor complex, and the pathway for deactivation. *FEBS Lett* 153:221–226
- Roelofs TA, Lee CH, Holzwarth AR (1992) Global target analysis of picosecond chlorophyll fluorescence kinetics from pea chloroplasts—a new approach to the characterization of the primary processes in photosystem II α units and β units. *Biophys J* 61:1147–1163
- Rohacek K, Bartak M (1999) Technique of the modulated chlorophyll fluorescence: basic concepts, useful parameters, and some applications. *Photosynthetica* 37:339–363
- Rutherford W, Govindjee, Inoue Y (1984) Charge accumulation and photochemistry in leaves studied by thermoluminescence and delayed light emission. *P Natl Acad Sci USA* 81:1107–1111
- Sayed OH (2003) Chlorophyll fluorescence as a tool in cereal crop research. *Photosynthetica* 41:321–330
- Schatz GH, Brock H, Holzwarth AR (1987) Picosecond kinetics of fluorescence and absorbency changes in photosystem II particles excited at low photon density. *P Natl Acad Sci USA* 84:8414–8418

- Schatz GH, Brock H, Holzwarth AR (1988) Kinetics and energetic model for the primary processes in photosystem II. *Biophys J* 54:397–405
- Schreiber U, Krieger A (1996) Two fundamentally different types of variable chlorophyll fluorescence in vivo. *FEBS Lett* 397:131–135
- Shampine LF, Reichelt MW (1997) The MATLAB ODE suite. *SIAM J Sci Comp* 18:1–22
- Shinkarev VP (2005) Flash-induced oxygen evolution in photosynthesis: simple solution for the extended S-state model that includes misses, double-hits, inactivation, and backward-transitions. *Biophys J* 88:412–421
- Sonneveld A, Rademaker H, Duysens LNM (1979) Chlorophyll *a* fluorescence as a monitor of nanosecond reduction of the photooxidized primary donor P_{680}^+ of photosystem II. *Biochim Biophys Acta* 548:536–551
- Stirbet A, Strasser RJ (2001) The possible role of pheophytine in the fast fluorescence rise OKJIP. In: Proceedings of the 12th international congress on photosynthesis (CD-ROM), S11–027, CSIRO Publishing, Collingwood
- Stirbet A, Govindjee, Strasser BJ, Strasser R (1998) Chlorophyll *a* fluorescence induction in higher plants: modelling and numerical simulation. *J Theor Biol* 193:131–151
- Strasser RJ, Srivastava A, Govindjee (1995) Polyphasic chlorophyll *a* fluorescence transient in plants and cyanobacteria. *Photochem Photobiol* 61:32–42
- Strasser RJ, Tsimilli-Michael M, Srivastava A (2004) Analysis of chlorophyll *a* fluorescence transient. In: Papageorgiou GC, Govindjee (eds) Chlorophyll *a* fluorescence: a signature of photosynthesis. Springer, Dordrecht, pp 321–362
- Trissl HW, Lavergne J (1995) Fluorescence induction from photosystem II - analytical equations for the yields of photochemistry and fluorescence derived from analysis of a model including exciton-radical pair equilibrium and restricted energy-transfer between photosynthetic units. *Aust J Plant Physiol* 22:183–193
- Trissl HW, Gao Y, Wulf K (1993) Theoretical fluorescence induction curves derived from coupled differential equations describing the primary photochemistry of photosystem II by an exciton radical pair equilibrium. *Biophys J* 64:974–988
- Vavilin DV, Tyystjarvi E, Aro EM (1998) Model for the fluorescence induction curve of photoinhibited thylakoids. *Biophys J* 75:503–512
- Vermeglio A (1977) Secondary electron transfer in reaction centers of *Rhodospseudomonas sphaeroides*: out-of-phase periodicity of two for the formation of ubiquinone and fully reduced ubiquinone. *Biochim Biophys Acta* 459:516–524
- Vernotte C, Etienne AL, Briantais JM (1979) Quenching of the system II chlorophyll fluorescence by the plastoquinone pool. *Biochim Biophys Acta* 545:519–527
- Vredenberg WJ (2000) A three-state model for energy trapping and chlorophyll fluorescence in photosystem II incorporating radical pair recombination. *Biophys J* 79:26–38
- Vredenberg WJ (2004) System analysis of photoelectrochemical control of chlorophyll fluorescence in terms of trapping models of Photosystem II: a challenging view. In: Papageorgiou GC, Govindjee (eds) Chlorophyll *a* fluorescence: a signature of photosynthesis. Springer, Dordrecht, pp 133–172
- Whitmarsh J, Bowyer JR, Crofts AR (1982) Modification of the apparent redox reaction between cytochrome-F and the Rieske iron-sulfur protein. *Biochim Biophys Acta* 682:404–412
- Wraight CA (1977) Electron acceptors of photosynthetic bacterial reaction centers Direct observation of oscillatory behavior suggesting two closely equivalent ubiquinones. *Biochim Biophys Acta* 459:525–531
- Zhu X-G (2004) Computational approaches to guiding biotechnological improvement of crop photosynthetic efficiency. Ph D thesis, the University of Illinois. Urbana, IL
- Zhu X-G, Ort DR, Whitmarsh J, Long SP (2004) The slow reversibility of photosystem II thermal energy dissipation on transfer from high to low light may cause large losses in carbon gain by crop canopies A theoretical analysis. *J Exp Bot* 55:1167–1175